American Journal of Botany 96(8): 1462–1486. 2009.

Evolution of lamina anatomy in the palm family (Arecaceae)[1]

James W. Horn,[2, 6] Jack B. Fisher,[2] P. Barry Tomlinson,[2–4] Carl E. Lewis,[2] and Karen Laubengayer[5]

[2]Fairchild Tropical Botanic Garden 11935 Old Cutler Rd., Coral Gables, Florida 33156 USA;
[3]The Kampong of the National Tropical Botanical Gardens, 4013 Douglas Road, Miami, Florida 33133 USA;
[4]Harvard Forest, Harvard University, Petersham, Massachusetts 01366 USA; and
[5]Department of Biological Sciences, Florida International University, Miami, Florida 33199 USA

The unique properties of tree building in Arecaceae strongly constrain their architectural lability. Potentially compensating for this limitation, the extensive diversification of leaf anatomical structure within palms involves many characters whose alternate states may confer disparate mechanical or physiological capabilities. In the context of a recent global palm phylogeny, we analyzed the evolution of 10 such lamina anatomical characters and leaf morphology of 161 genera, conducting parsimony and maximum likelihood ancestral state reconstructions, as well as tests of correlated evolution. Lamina morphology evolves independently from anatomy. Although many characters do optimize as synapomorphic for major clades, anatomical evolution is highly homoplasious. Nevertheless, it is not random: analyses indicate the recurrent evolution of different cohorts of correlated character states. Notable are two surface layer (epidermis and hypodermis) types: (1) a parallel-laminated type of rectangular epidermal cells with sinuous anticlinal walls, with fibers present in the hypodermis and (2) a cross-laminated type of hexagonal cells in both layers. Correlated with the cross-laminated type is a remarkable decrease in the volume fraction of fibers, accompanied by changes in the architecture and sheath cell type of the transverse veins. We discuss these and other major patterns of anatomical evolution in relation to their biomechanical and ecophysiological significance.

Key words: Arecaceae; correlated evolution; epidermis; homoplasy; hypodermis; lamina anatomy; leaf biomechanics; macroevolution; palm phylogeny; venation architecture.

A recent global phylogeny of Arecaceae, with nearly complete sampling at the generic level (Asmussen et al., 2006) provides many breakthroughs in the inference of relationship for taxonomically enigmatic groups within palms and resolves for the first time a comprehensive and robust macrosystematic hypothesis for the family. It serves as the definitive basis for current palm classification, in which this family of 183 genera and over 2500 species is divided into five, successively sister subfamilies: Calamoideae, Nypoideae, Coryphoideae, Ceroxyloideae and Arecoideae (Dransfield et al., 2005, 2008b; Fig. 1). Of equal importance, it opens up the opportunity for comparative analyses of the wealth of structural data generated by the long and sustained research interest these monocot giants have attracted and continue to attract (Baker and Zona, 2006). Inspired by surveying the lamina anatomy of all palm genera for an updated account of the systematic anatomy of Arecaceae, our study aims at revealing the major patterns present in the evolution of lamina anatomy within palms.

Providing further impetus to these research endeavors is the inherent interest in the construction of palms, which is interpretable within the context of the organization of monocot body plan (e.g., development entirely through primary growth), yet also unique in the way palms use this body plan to attain tree proportions (Tomlinson, 1990). If the tree stature of palms is achieved through maximizing efficiency of the developmental, mechanical, and physiological properties the monocot body plan (Tomlinson, 2006), it is the key innovation of their unique mode of compound leaf development through plication formation that has unlocked the potential for gigantism in this system. Plication confers the developmental capability for gigantism in producing a repeating series of folds through differential growth (Dengler et al., 1982; Kaplan et al., 1982) and by precise segment separation through abscission and cell separation along segment margins by apoptosis (Nowak et al., 2007, 2008). Relatively dramatic increases in lamina surface area can be achieved with maximal efficiency in packing prior to leaf expansion. Plication also gives a mechanically efficient shape to palm leaves, conferring to them a high second moment of area (i.e., resistance to bending forces; Niklas, 1992; King et al., 1996). Consequently, the architecture of the two basic forms of palm leaves—pinnate and palmate—conforms with relative precision to abstracted models of leaves based on engineering theory (Niklas, 1999). In synergy with these outcomes of plication, the extensive deployment of mechanical tissues in the leaf base, axis, and system of ribs that enervate the lamina, facilitates the capability for gigantism.

The production of large leaves requires the production of a stem of proportionally large girth for vascular supply (Tomlinson,

[1] Manuscript received 26 November 2008; revision accepted 1 April 2009.

The authors thank B. Whitney for technical assistance, C. Asmussen for supplying the data matrix used in Asmussen et al. (2006), W. J. Baker for dried leaf samples from Kew (K), R. Dirig for dried leaf samples from Cornell (BH), M. Bourell for leaf samples from the San Francisco Botanical Garden, and H. Forbes for leaf samples from University of California Botanical Garden at Berkeley. P. Griffith generously allowed full access to the collections of the Montgomery Botanical Center throughout the course of this study. C. Jones Leiva, curator of the living palm and cycad collections at FTBG, facilitated our collection efforts with unstinting patience. L. Woodbury and FTBG volunteers provided herbarium support. Research was supported in part by NSF award 0515683 and the Crum Professorship in Tropical Botany of the National Tropical Botanical Garden.

[6] Author for correspondence (e-mail: hornj@si.edu); present address: Department of Botany and Laboratories of Analytical Biology, Smithsonian Institution, P.O. Box 37012, NMNH MRC-0166, Washington, D.C. 20013-7012 USA

doi:10.3732/ajb.0800396

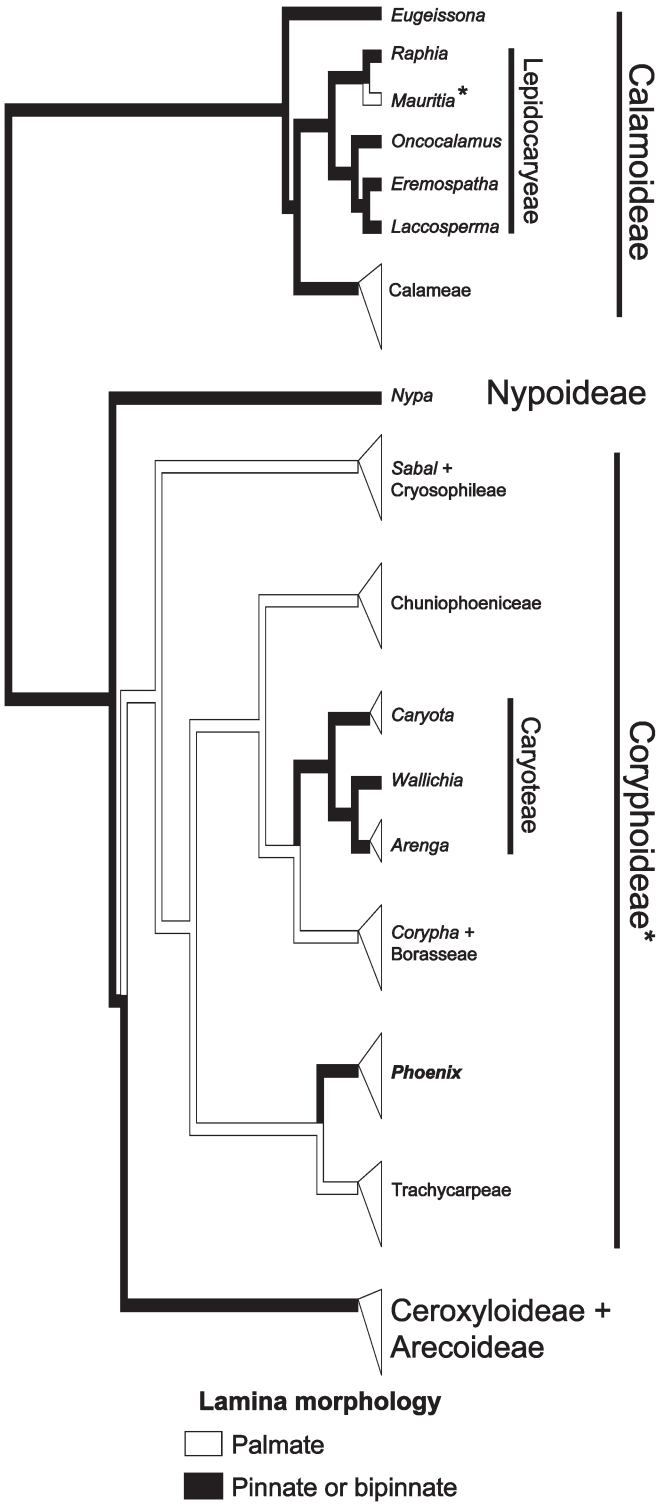

Fig. 1. Summary phylogeny of Arecaceae, showing evolution of lamina morphology. The tree represents the strict consensus of a set of 100 trees, with many nodes collapsed; outgroup taxa not shown. Parsimony reconstruction of lamina morphology optimizes onto all trees with four steps. Independent gains of palmate leaves (*) are indicated for subtribe Mauritiinae (represented here by *Mauritia* only) and Coryphoideae. Independent reversals to pinnate leaves are indicated for Caryoteae and *Phoenix*. Maximum likelihood reconstruction of this character is identical to the results shown (online Appendix S25).

2006). Matched with a nearly solid cylinder of vascular fibers toward their periphery (which increase in thickness, and correspondingly, rigidity, with age), palm stems possess the physical and material properties to attain tree stature (Rich, 1987). The mechanical characteristics of palms as tree systems are further enhanced by a counterbalanced crown geometry that is fully integrated into the vascular architecture of the stem (Niklas, 1992). Tree building in palms therefore results from an intricately organized mode of construction between the leaves and the stem that is predicated upon leaf gigantism.

Yet if palm tree building is successful in this way, it poses considerable constraints upon the extent to which these trees can dynamically respond to changes in their environment and the extent to which morphological novelty can be introduced into this system. Owing to their fixed vascular architecture, palm stems are almost incapable of aerial branching. Further, palm leaves, though perhaps the most outstanding monocot examples of foliar analogs with branches (Givnish, 1979), are comparatively inflexible developmentally, having little ability to undergo spatial adjustment within the crown (Zobel and Liu, 1980). Also nearly lacking is a capability to reorient or abscise pinnae and segments within a mature leaf. With such severe limitations on the lability of external form, it may seem paradoxical that palms achieved any appreciable extent of systematic or ecological diversity whatsoever.

That palms undoubtedly are a species-rich and ecologically ample clade is, we suggest, in substantial part due to diversification in their leaf anatomy. Functional significance is clearly attributable to many lamina anatomical characters that show obvious variation; diversification here may effectively compensate for the limitations discussed. Significantly, such variation appears to be largely decoupled from the morphology of the lamina. Compare Fig. 2B, I, and K, all from species with pinnate leaves. Although the leaves of these species of *Dypsis*, *Butia*, and *Ceroxylon* do differ somewhat in external form, the degree of this difference is not suggestive of their remarkable anatomical disparity. The lamina of these taxa have major anatomical differences in the presence and distribution of fibers (Fig. 2B, I, K). Because fibers assume much of the load-bearing capacity of the lamina (Schwendener, 1874; Vincent, 1982, 1991), these structural differences may be expected to reflect corresponding differences in biomechanical attributes. The symmetry of the lamina histology also varies among these three species. *Dypsis* and *Ceroxylon* have a distinctly dorsiventral arrangement of tissues (Fig. 2B, K), while *Butia* exemplifies isobilateral lamina histology, in which the adaxial and abaxial leaf surfaces and mesophyll are alike, so that (disregarding the polarity of the vascular bundles) they are about mirror-image equivalents (Fig. 2I). Again, varying functional attributes likely accompany this major structural difference, because isobilateral leaves, with stomata and palisade mesophyll positioned at both leaf surfaces, can maximize the distribution of carbon dioxide (Mott et al., 1982; Slaton and Smith, 2002) and light (Vogelmann and Martin, 1993; Vogelmann et al., 1996) within the lamina. In high light environments, isobilateral leaves are therefore capable of greater rates of photosynthesis per unit biomass than their dorsiventral counterparts (Smith et al., 1997).

These and other characters, involving the epidermis, hypodermis, and transverse veins, collectively constitute much of the most readily perceptible anatomical variation within palm leaves. While Tomlinson (1961, 1990) located substantial systematic significance in many of these characters, he proposed

that their principal interest to palm evolution is rather that they form complex trait associations that may have multiple, independent origins within the family. We here document this suggestion more objectively.

Patterns of recurrent evolution among structurally integrated character associations, often difficult to discern using phylogenetic and intuitive analyses of discrete morphological features, are of considerable macroevolutionary importance as they suggest, on the one hand, their combined functional significance, and on the other, the effect of developmental bias or canalization upon the variation available for selection (Brakefield, 2006). A critical first step toward a synthesis of evolution, development, and function is therefore the identification and evolutionary analysis of such repeatedly evolving character cohorts (Jabbour et al., 2008). The use of molecular phylogenetic data are essential in this regard because they provide an independent framework for the reconstruction of ancestral states, making possible the explicit dissection and quantification of structural homoplasy (Donoghue and Sanderson, 1994; Donoghue and Ree, 2000). Furthermore, they permit the use of comparative methods to test correlated transitions between two characters in evolution (Givnish et al., 2005). Using this approach to analyze the evolution of the anatomy of the palm leaf lamina, our goals are to (1) examine the evolution of 10 major characters of greatest structural, and potentially functional, significance in the context of a new phylogenetic hypothesis for palms (Asmussen et al., 2006); (2) test for correlated evolutionary transitions between all pairwise combinations of nine of these characters, as well as lamina morphology type, and (3) synthesize our results in the context of contemporary studies on leaf biomechanics and ecophysiology. In doing so, we present a set of hypotheses regarding the evolution of structure/function relationships that can serve as a starting point for more detailed, empirical studies on the comparative biomechanics and ecophysiology of palm leaves.

MATERIALS AND METHODS

Taxa examined—One hundred seventy-eight palm species, representing 161 of the 183 genera of palms recognized by Dransfield et al. (2008b) were investigated. The full nomenclature of species sampled is given in Appendix 1. These species represent an almost exact parallel with those analyzed in the global palm phylogeny of Asmussen et al. (2006). Lamina material of mature plants was collected from the living collections of Fairchild Tropical Botanic Garden (Florida), the Montgomery Botanical Center (Florida), National Tropical Botanic Garden (Hawaii), San Francisco Botanical Garden, and University of California Botanical Garden at Berkeley, as well as from herbarium specimens lodged at BH, FTG, and K for taxa not in cultivation. For a few genera, species substitutions were made where no material was available for structural investigation of the species sampled by Asmussen et al. (2006). In the current study, observations from at least three species in such genera (*Licuala*, *Metroxylon*, *Ravenea*, and *Salacca*) were substituted to ensure uniformity of the character state codings (see Appendix 1, species in boldface). Where we substituted a species to serve as an alternate for a particular species within a genus where Asmussen and colleagues sampled more than one taxon, relevant recent taxonomic treatments informed our choice of a close relative; hence, *Orania trispatha* was substituted for *O. ravaka*. Dransfield and Beentje (1995) suggested a close relationship between these two taxa as among the three Madagascan species of *Orania*, just these two show distichous phyllotaxy—a rare character state within palms. Character states for *Masoala* were coded from *M. madagascariensis*.

Sectioning, staining, and photography—Because we sampled the palm family extensively, we needed simple and rapid methods for processing abundant material, as in Tomlinson (1961).

From mature, adult foliage, lamina samples were collected from a pinna or segment located at about the middle of the leaf blade. A portion from the midlength of such pinnae or segments was removed and fixed in formalin-acetic acid-alcohol (FAA; 10 parts 40% formaldehyde, 85 parts 70% ethanol, 5 parts glacial acetic acid). Surface preparations were made by scraping away unwanted tissue with a blunt scalpel from a sample laid flat on a wet tile, ideally until only epidermal and hypodermal tissues were left (Fig. 3). Transverse (TS) and longitudinal sections (LS) were cut with a sliding microtome at a thickness of 20–30 μm, after preliminary overnight soaking of material in 50% hydrofluoric acid (HF). Microscope preparations were made of either unstained sections or sections bleached for 15–20 min in 50% commercial bleach (sodium hypochlorite), washed in water, and stained in 0.02% toluidine blue O. Preparations were mounted in commercial corn syrup (Karo ACH Food Co., Memphis, Tennessee, USA), which hardens over time to make permanent preparations, whose faded stain can be easily restored subsequently by soaking off the cover glass in warm water. This approach eliminates the lengthy process of dehydration and double staining with its consequent artifacts and retains material in a more natural hydrated condition.

Permanent whole mounts were made of segments cleared in 5% NaOH in a covered Petri dish and warmed to 55°C in an oven for 1–3 d or until relatively clear. The parts were washed, bleached in commercial Na hypochlorite solution, washed again, dehydrated in 50% ethanol, stained with 1% safranin in 50% ethanol, destained and dehydrated in an ethanol series ending with xylene or Citrosolve, and mounted in Permount (Fisher Scientific, Fairlawn, New Jersey, USA) on a 50 × 75 mm slide (Fig. 4D–K).

Photography was done using a Coolpix 4500 digital camera (Nikon, Tokyo, Japan). The image was adjusted for contrast and color level in Adobe (San Jose, California, USA) Photoshop but pixels within the object of concern were otherwise untouched. Background areas outside the object were cleared to improve the clarity of the image.

Structural data—Anatomical data were collected from direct observations of longitudinal and transverse sections, epidermal scrapes, and leaf clearings. Observations were typically based upon a single sample for each species studied. Among palms, character state data for *Sclerosperma* alone was coded from the description and illustrations provided by Tomlinson (1961). Outgroup taxa were coded from specimens listed in Appendix 1, as well as from Fahn (1954, 1961), Metcalfe (1960), and Tomlinson (1969).

Data were collected for one morphological character, i.e., pinnate vs. palmate leaf shape, and 10 anatomical characters. In our initial survey, we found that these features showed a correspondence to taxonomic groups and appeared to be associated with one another in various ways in agreement with the information presented earlier in Tomlinson (1961, 1990). We chose those characters because of their perceived biological significance as major structural features of the palm lamina, which is further elaborated upon in the Discussion. Coding of states for the single morphological character, lamina morphology type (pinnate vs. palmate), follows Dransfield et al. (2008b).

Anatomical characters are as follows, with their character states listed in the Results: (1) epidermal cell shape outline in surface view, (2) adaxial hypodermal cell shape outline in surface view, (3) adaxial epidermal anticlinal cell wall contour in surface view, (4) transverse vein sheath cell type, (5) transverse vein architecture in surface view, (6) adaxial subepidermal fibers, (7) nonvascular fiber bundles free in mesophyll, (8) nonvascular fiber bundles attached to surface layer as a regularly repeating series, (9) continuity of longitudinal veins with adaxial surface layer (coded as both a binary and multistate character, respectively 9a and b), (10) symmetry of lamina histology.

We present the complete character matrix in Appendix S1 (see Supplemental Data with the online version of this article).

Phylogenetic data—The set of trees used as the analytical framework for this study is based upon the maximum parsimony (MP) analysis of Asmussen et al. (2006), who used sequence data from four plastid loci for 178 palm species and 10 outgroup taxa. They presented the most comprehensively sampled analysis of palm family phylogeny to date. Their combined analysis recovered a large set of MP trees that show appreciable but strongly localized topological conflict. Thus, the strict consensus tree is generally well resolved, but with nearly complete polytomies summarizing relationships within tribe Cryosophileae of subfamily Coryphoideae, and, notably, at both the backbone of Arecoideae and the large tribe Areceae. The following analytical strategy therefore attempts to take into account this topological uncertainty through a sensitivity analysis by conducting all analyses over 100 randomly sampled MP trees. That the sampled set of 100 trees serves as an adequate proxy for the full set of MP trees is justifiable on the basis that the strict consensus of

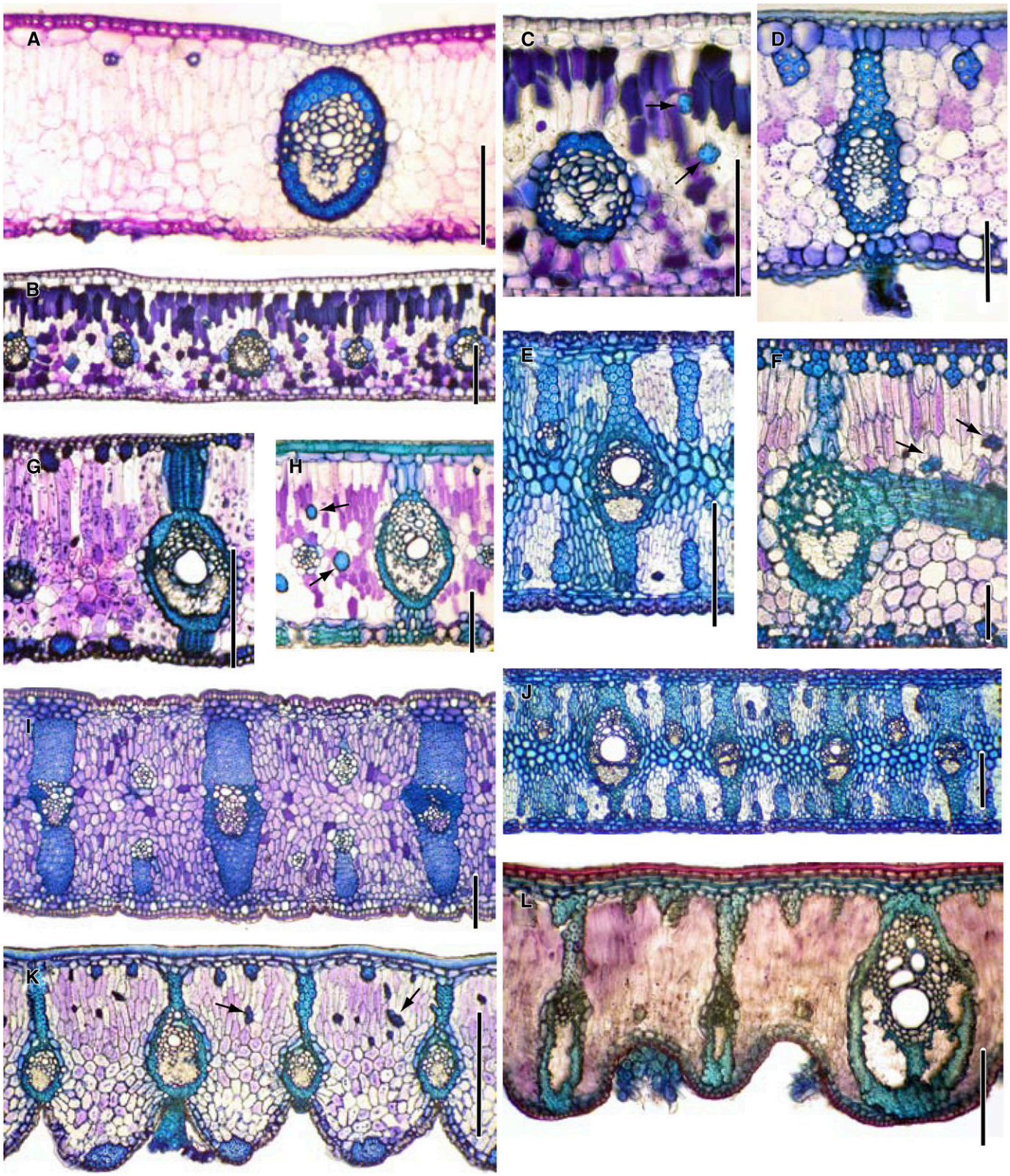

Fig. 2. Lamina in transverse section, adaxial surface oriented toward top of page; all stained with toluidine blue. A–C. Vascular bundles without bridges. (A) *Arenga microcarpa.* (B) *Dypsis lutescens.* (C) *Dypsis lutescens*. D, E. Vascular bundles with fiber bridges. (D) *Oraniopsis appendiculata*. (E) *Bismarkia nobilis*. F–H. Vascular bundles with sclereid bridges. (F) *Metroxylon vitiense*. (G) *Mauritiella armata*. (H) *Nypa fruticans*. I, J. Examples of convergent evolution of isobilateral lamina anatomy. (I) *Butia capitata* in Arecoideae (Cocoseae: Attaleinae). (J) *Bismarkia nobilis* in Coryphoideae (Borasseae). K, L. Examples of convergent evolution of fiber bridges and stomatal furrows in leaves of Andean palms. (K) *Ceroxylon quindiuense* in Ceroxyloideae (Ceroxyleae). (L) *Parajubaea cocoides* in Arecoideae (Cocoseae: Attaleinae). Arrow, free fiber bundle. Scale bars: F, 50 μm; A–E, G–K, 100 μm; J, K, L, 200 μm.

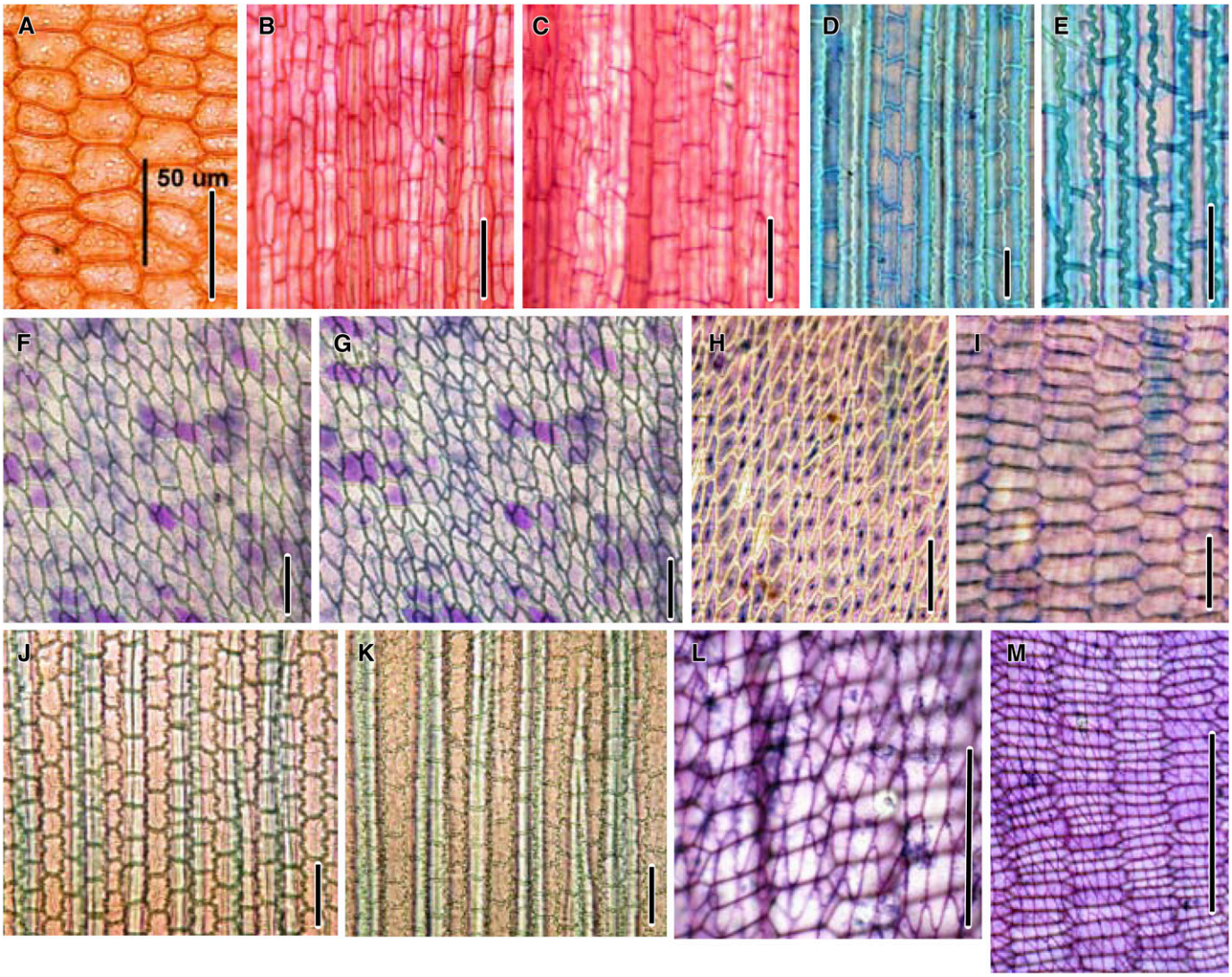

Fig. 3. Epidermis and hypodermis of adaxial surface in surface view. (A) *Juania australis,* nonelongated, hexagonal epidermal cells, stained with Sudan IV. B, C. *Trachycarpus fortunei*, elongated, rectangular epidermal cells with straight walls; rectangular hypodermal cells. (B) Epidermis; (C) same position and magnfication with different focal plane to show hypodermis; both in safranin. D, E. *Rhapis excelsa*, elongate rectangular epidermal cells with sinuous walls; same preparation with different magnification to show (D) hypodermis and (E) epidermis; both in toluidine blue. F, G. *Dypsis lutescens*, oblique hexangular epidermal and hypodermal cells. (F) Epidermis; (G) same position and magnification with different focal plane to show hypodermis; both in toluidine blue. H, I. *Arenga microcarpa*, oblique and elongated hexagonal cells of epidermis and hypodermis; (H) Epidermis of fresh specimen, nuclei visible; (I) same position and magnfication with different focal plane to show hypodermis; both in toluidine blue. J, K. *Plectocomia muelleri*, rectangular epidermal cells with sinuous walls and hypodermis with fibers (light vertical bands) and rectangular cells. (J) Epidermis; (K) same position and magnfication with different focal plane to show hypodermis; both in toluidine blue. (L) *Reinhardtia gracilis*, oblique and hexagonal (spindle-shaped) epidermal cells with transverse hexagonal hypodermal cells; in toluidine blue. (M) *Socratea exorrhiza*, longitudinal and hexagonal epidermal cells with transverse hexagonal hypodermal cells; in toluidine blue. Scale bars: A–K, 50 μm; L, 100 μm; M, 200 μm.

the 100 trees shows an almost identical topology to that of the full set of MP trees. Increased resolution in the strict consensus of the 100 sampled trees is restricted to the sister pairing of *Dypsis* and *Marojejya* within tribe Areceae, and the positioning of *Phytelephas macrocarpa* and *Ammandra decasperma* as successively sister to *Aphandra natalia* + *Phytelephas aequatorialis* in tribe Phytelepheae.

We obtained the data matrix analyzed by Asmussen et al. (2006) and replicated a set of over 41 000 MP trees (length = 4176) using the program PAUP* version 4.0b10 (Swofford, 2002). From this set of optimal trees, 100 were randomly sampled; polytomies inherent in the topologies were randomly resolved. Branch lengths of these trees were optimized in PAUP* using a full likelihood evaluation under a GTR + I + Γ substitution model, as selected by the Akaike information criterion (AIC) in the program Modeltest version 3.7 (Posada and Crandall, 1998). Starting branch lengths were estimated using the least squares method to avoid the calculation of negative branch lengths.

Ancestral state optimizations and comparative analysis—All evolutionary analyses were conducted using the program Mesquite version 2.5 (Maddison and Maddison, 2008). Parsimony optimizations for all characters were conducted on the strict consensus tree of Asmussen et al. (2006) under both the soft and hard polytomy options to establish for each character the minimal and maximal number of possible changes. All other analyses use the set of 100 trees described. Branch lengths of zero were set to the minimum length recognized by Mesquite (1×10^{-7}; Case et al., 2008). Ancestral state reconstructions were

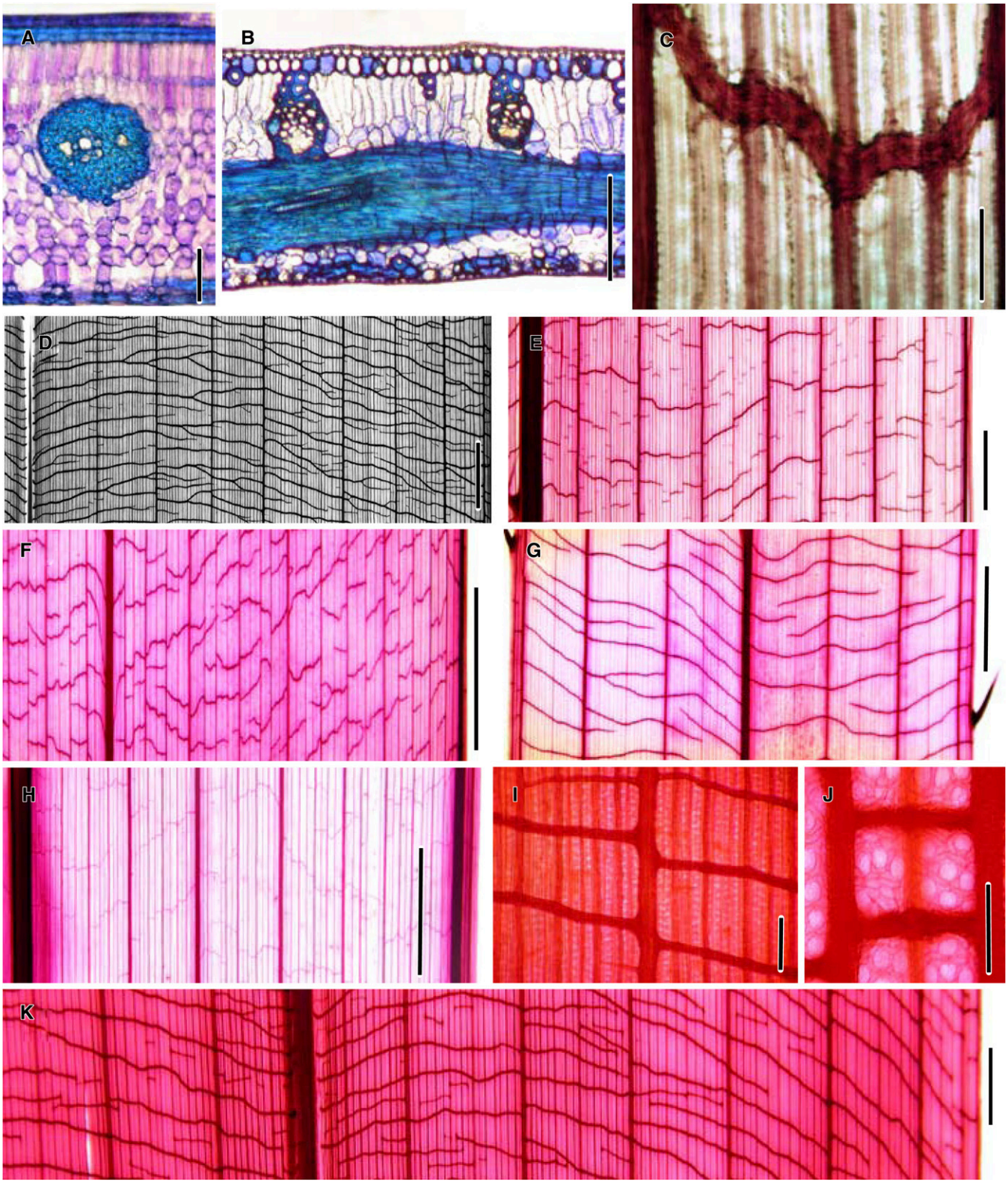

Fig. 4. Transverse veins of lamina. A, B. Lamina sections with adaxial surface toward top of page. (A) *Metroxylon vitiense*, transverse vein in TS, lamina cut in LS; in toluidine blue. (B) *Borassodendron machadonis*, transverse vein in LS, longitudinal veins in TS; in toluidine blue. C–K Adaxial surface views of cleared specimens. (C) *Zombia antillarum*; in Bismark brown. (D) *Borassodendron machadonis*; in black and white. (E) *Metroxylon vitiense*, midrib on left; in safranin. (F) *Zombia antillarum*, margin on right; in safranin. (G) *Laccosperma secundiflorum*, margins right and left, midrib center, in safranin. (H) *Dypsis lutescens*, margin right, in safranin. (I) *Borassus heineanus*; in safranin. (J) *Borassus flabellifer*; in safranin. (K) *Attalea allenii*, midrib left center; in safranin. Scale bars: A, 50 μm; B, 100 μm; C, J, 200 μm; I, 250 μm; E, 1 mm; H, K, 2 mm; D, F, G, 5 mm.

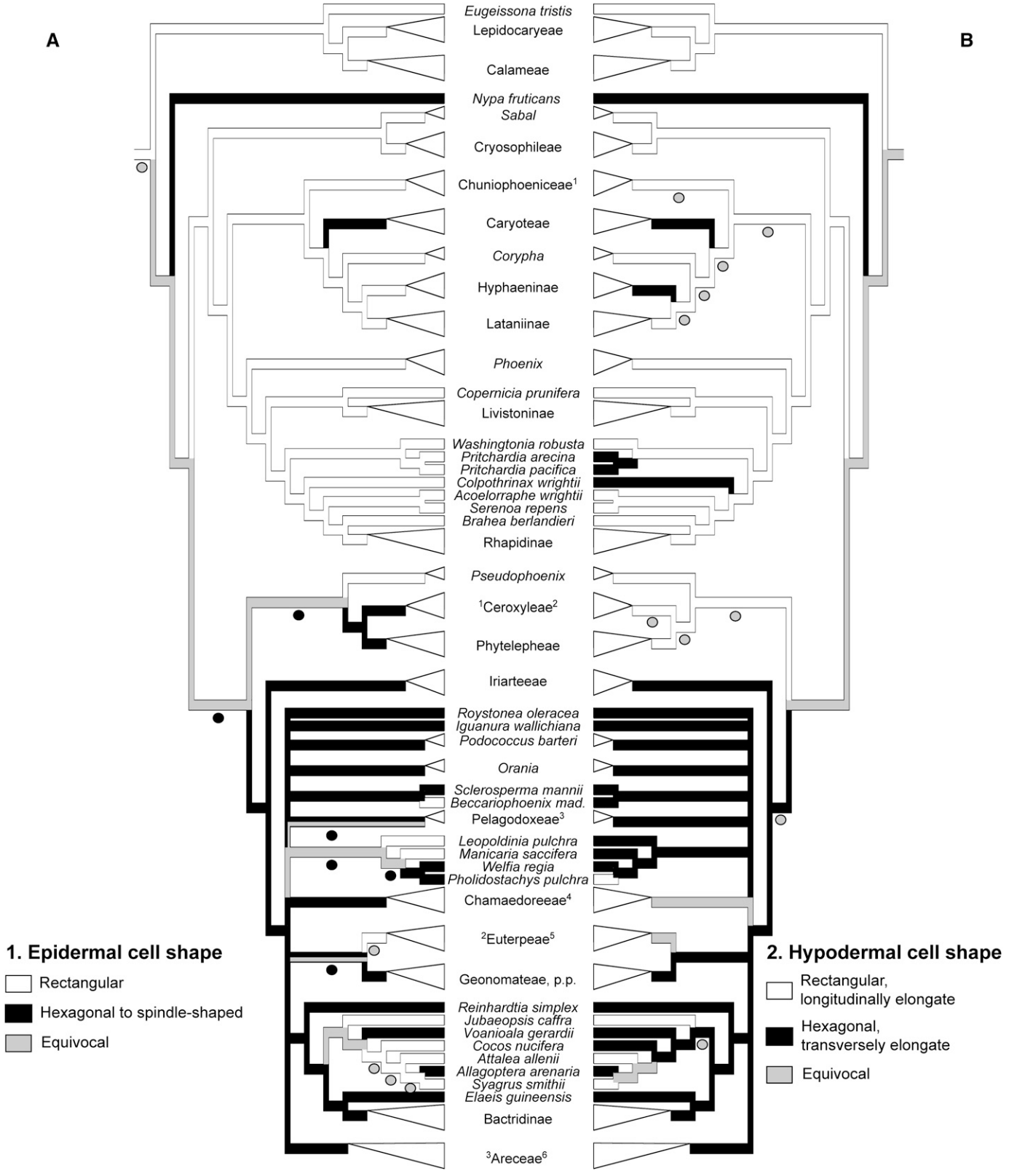

Fig. 5. Summary of parsimony reconstructions of ancestral states for 100 trees displayed onto strict consensus for (A) adaxial epidermal cell shape, surface view and (B) adaxial hypodermal cell shape, surface view. Summary of maximum likelihood reconstructions indicated in circles below branches that differ from parsimony results. (A) Epidermal cell shape optimizes onto 100 trees with 19 steps, all changes within palms. Superscript to left of a taxon denotes state changes within collapsed clades: [1] →0 *Oraniopsis*; [2] 0: Euterpeae exclusive of *Neonicholsonia*(→1); [3] 0: *Calyptrocalyx*, *Cyrtostachys*, *Linospadix* + *Laccospadix*, Oncospermatinae, *Rhopaloblaste*. (B) Hypodermal cell shape optimizes onto 100 trees with 29 steps, 27–28 within palms.

conducted for each character using both parsimony and likelihood methods (Schulter et al., 1997). Parsimony character steps were collected from all 100 trees for each character by assessing their value for a single tree (i.e., Current tree in Mesquite), then using the Step Through Trees command to collect the full set of values. Maximal and minimal values of forward and reverse character state changes were gathered for the clade of Arecaceae using the Summarize Changes in Selected Clade command, using all 100 trees, with the maximum number of mappings sampled for each character on each tree set to 50. Parsimony reconstructions for a given character on each of the 100 trees were summarized onto the strict consensus of the 100 trees using the Trace Character Over Trees command.

Likelihood optimizations were conducted using the StochChar package (Maddison and Maddison, 2006) in Mesquite. Asymmetry likelihood ratio tests were conducted for all characters (except multistate 9b) across all trees using the same facilities in Mesquite as outlined for gathering parsimony character step data. The asymmetrical two-parameter model (AsymmMk) yielded significantly better likelihoods at the threshold of $P < 0.05$ for character 7, $P < 0.01$ for character 4, and $P < 0.001$ for characters 1 and 10. The single parameter model (Mk1; Lewis, 2001) was used for likelihood optimizations of all other characters. Likelihood reconstructions for a given character on each of the 100 trees were summarized onto the strict consensus of the 100 trees using the Trace Character Over Trees command with the likelihood decision threshold set to 2.0.

Tests of phylogenetic independence between two discrete character states employed the Pagel 94 analysis, a component of the Correl package (Midford and Maddison, 2006) in Mesquite. This analysis is a modification of the method originally described by Pagel (1994) because here the four-parameter model is a special case of the eight-parameter model. Because the goal of this test was to evaluate hypotheses of structural correlation within palms, outgroup branches were pruned from all trees prior to analysis. Calamoideae were therefore used to root these trees because their relationship as sister to all other palms is strongly supported (Asmussen et al., 2006). Pairwise analyses of characters were conducted by stepping through the set of 100 trees, calculating likelihood values for the eight-parameter model with 10 search iterations, and collecting a complete set of log likelihood ratios for all trees examined. Significance of the likelihood ratio test statistics ($-2\ln L$) was assessed against a χ^2 distribution with four degrees of freedom. To be conservative in our interpretations, the hypothesis of phylogenetic independence was rejected only when the test statistics for the 100 trees were all significant at the $P < 0.01$ level.

RESULTS

Ancestral state reconstructions—Figures 1 and 5–10 for ancestral state reconstructions represent a summary of both parsimony and likelihood reconstructions over the set of 100 trees displayed onto the strict consensus of these 100 trees. The 10 outgroup taxa are pruned at the basal node of palms and not shown. We present reconstructions of characters 1–8 in mirror tree format (Figs. 5–8) to make apparent the pattern of correlated evolution between the characters in each pair (discussed later; Table 1). Necessarily, not all 178 palm taxa could be illustrated; hence, most terminal clades, representing current concepts of tribes or subtribes, are shown artificially collapsed to their basal node. We represent character state changes within collapsed clades shown in Figs. 5–9 in a concise way using superscript numbers. These numbers are positioned to the side of the taxon name adjacent to the tree to which they correspond. Within the figure legend, an arrow indicates the direction of unambiguous state transitions. For collapsed terminals that represent polytomies and those with an equivocal reconstruction at the basal node, we provide a summary of state variation without inferring polarity. Parsimony and likelihood reconstructions showing all palm and outgroup taxa are presented in Appendices S2–S25 (see Supplemental Data with online version of this article; parsimony: S2–S13; maximum likelihood: S14–S25).

Parsimony and likelihood ancestral state reconstructions for each character are congruent to the extent that there are no instances where opposing states are unambiguously reconstructed at a node. Discrepancies in state reconstructions at a given node are infrequent for most characters and occur as instances where one of the two optimization methods yielded an equivocal reconstruction. At the basal node of the family and at least the deepest two internal nodes within the clade of palms without Calamoideae, likelihood reconstructions of all anatomical characters are uniformly equivocal. This is unsurprising given the relatively great disparity in branch lengths between the very long branches of the outgroup taxa and those within palms.

The evolution of all anatomical characters and leaf type is substantially homoplasious, with each showing a complex pattern of state gains and losses. We indicate below the minimum and maximum values for the number of parsimony steps required to optimize each of the anatomical characters onto the strict consensus tree of Asmussen et al. (2006; under each character as "min" and "max"). A comparison of these values with those obtained from optimizations of each character onto each of the 100 fully resolved trees demonstrates that, for all characters, the values for the 100 trees are near or equivalent to the maximum number of possible steps. We provide summaries of parsimony state transitions within palms for each anatomical character listed below, indicating the minimum (min) and maximum (max) number of gains (0→1) and losses (1→0) inferable. These summaries indicate that independent gains of sinuous anticlinal cell walls (character 3, Fig. 6A), adaxial subepidermal fibers (character 6, Fig. 6B), and isobilateral lamina histology symmetry (character 10, Fig. 10) are always more numerous than reversals. The two types of transverse vein sheathing cells (character 4, Fig. 7A) show an equivalent number (= 6) of independent state gains and reversals to favoring eight gains of sclerotic parenchyma and four reversions back to many layers of fibers. The evolution of nonvascular fiber bundles free in the mesophyll (character 7, Fig. 8A) shows a unique pattern among characters examined as all reconstructions strongly favor fiber bundle losses over gains. State transition summaries of other characters indicate no clear general directionality in their evolution (disccused later).

Leaf type: Palmate leaves evolved twice within the family, with two independent reversals back to the pinnate state (Fig. 1; Appendices S13, S25).

Epidermal cell shape outline in surface view (character 1; Fig. 5A; Appendices S2, S14): 0 = rectangular; 1 = hexagonal or spindle-shaped. In surface view, epidermal cell shape ranges from elongated rectangular (Fig. 3B, D, E, J) to hexagonal and isodiametric (Fig. 3A), or hexagonal with oblique and longitudinal elongation into a spindle (Fig. 3F, H, L).

Epidermal cell shape optimizes onto each of the 100 trees with 19 steps, all changes within palms. State transitions within palms: 0→1 min = 4, max = 11; 1→0 min = 8, max = 15.

←

Superscript to right of a taxon denotes state change(s) within collapsed clades: [1] →1 *Kerriodoxa* + *Nannorrhops*; [2] →1 *Juania*, *Oraniopsis*; [3] →0 *Sommieria*; [4] 0: all except *Hyophorbe*; [5] 0: all except *Euterpe*; [6] 0: *Brassiophoenix*, *Calyptrocalyx*, *Cyrtostachys*, *Linospadix* + *Laccospadix*, *Loxococcus*, *Rhopaloblaste*.

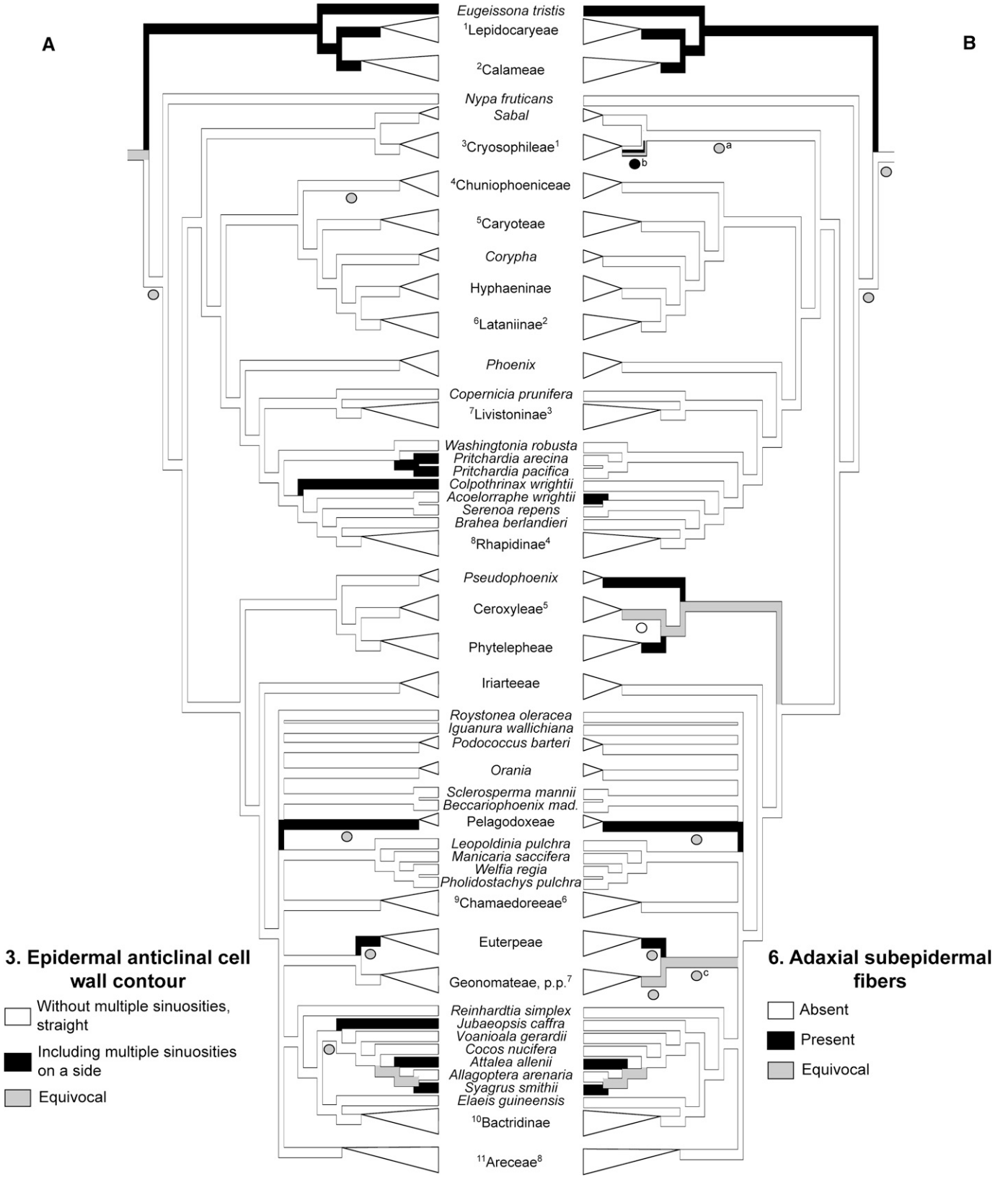

Fig. 6. Summary of parsimony reconstructions of ancestral states for 100 trees displayed onto strict consensus for (A) epidermal anticlinal cell wall contour, surface view, and (B) Adaxial subepidermal fibers. Summary of maximum likelihood reconstructions indicated in circles below branches that differ from parsimony results. (A) Epidermal anticlinal cell wall contour optimizes onto 99 trees with 29 steps, one tree with 28 steps; all changes but one are within palms. Superscript to left of a taxon denotes state change(s) within collapsed clades: [1] →0 *Laccosperma*; [2] →0 *Korthalsia*; [3] 1: *Itaya*, *Schippia*,

Optimization onto strict consensus min = 16 steps, max = 19 steps. As shown in Fig. 5A, hexagonal to spindle-shaped cells evolved independently from other palms in tribe Caryoteae (Coryphoideae). Maximum likelihood (ML) optimizations unambiguously reconstruct this state more broadly, assigning it to the both the basal nodes of Ceroxyloideae and Ceroxyloideae + Arecoideae. Notable reversions back to rectangular cells occur in *Pseudophoenix* (ML), once at or near the base of Euterpeae (Arecoideae), and at least once in Attaleinae (Arecoideae: Cocoseae; clade inclusive of *Jubaeopsis* and *Syagrus*).

Adaxial hypodermal cell shape outline in surface view (character 2; Fig. 5B; Appendices S3, S15): 0 = quadrangular; 1 = hexangular, transversely extended. The shape of the adaxial hypodermis in surface view ranges from rectangular and longitudinally elongate (Fig. 3C, D; including elongate fibers or elongate sclerenchyma, Fig. 3 K), to hexagonal and transversely elongate (Fig. 3G, I, L, M).

Hypodermal cell shape optimizes onto 100 trees with 29 steps, 27–28 within palms. State transitions within palms: 0→1 min = 9, max = 15; 1→0 min = 12, max = 19. Optimization onto strict consensus min = 25 steps, max = 29 steps. Figure 5B shows a similar pattern of state transitions to that of character 1, but with parsimony reconstructions indicating independent gains of transversely elongate, hexagonal cells in several lineages within Coryphoideae in addition to Caryoteae. Another notable difference is that parsimony reconstructions unambiguously assign contrasting states to the basal nodes of Ceroxyloideae and Arecoideae. At least one reversal is necessary to reconstruct this character for Chamaedoreeae (Arecoideae) because all but *Hyophorbe* possess a very weakly developed hypodermis of rectangular to about square cells, as seen in surface view.

Adaxial epidermal anticlinal cell wall contour in surface view (character 3; Fig. 6A; Appendices S4, S16): 0 = straight, not including multiple sinuosities; 1 = including multiple anticlinal sinuosities. The anticlinal wall ranges from straight (Fig. 3A, B, F, H) to sinuous, especially near the cuticle (Fig. 3D, E, J).

Epidermal anticlinal cell wall contour optimizes onto 99 trees with 29 steps, one tree with 28 steps; all changes but one are within palms. State transitions within palms: 0→1 min = 21, max = 26; 1→0 min = 2, max = 6. Optimization onto strict consensus min = 25 steps, max = 29 steps. Sinuous anticlinal walls of epidermal cells are gained many times throughout the family, with most changes concentrated toward the tips of the tree. Calamoideae are a major exception; sinuous walls optimize as the ancestral state for the subfamily. Reversals back to straight walls, which are uncommon, are concentrated within Calamoideae (Fig. 6A). Arecoideae have notable gains of sinuous walls in Pelagodoxeae and Euterpeae. Multiple gains and losses may be inferred for Attaleinae. Characters 3 and 6 show significant correlated evolution; pairing them in mirror tree format allows the reader to explore this visually.

Transverse vein sheath cell type (character 4: Fig. 7A; Appendices S5, S17): 0 = many layers of fibers; 1 = one or two layers of short-celled sclerenchyma. The transverse veins of many taxa have a sheath of fibers (Fig. 4A, B) forming a smooth surface to the vein as seen in clearings (Fig. 4I, J), while veins in other taxa have a sheath of short, irregular sclereids that form an uneven surface to the vein (Fig. 4C). We did not code a condition found in some taxa in which sheathing fibers extend into the adjacent mesophyll.

Transverse vein sheath cell type optimizes onto 100 trees with 14 steps, 12 within palms. State transitions within palms: 0→1 min = 6, max = 8; 1→0 min = 4, max = 6. Optimization onto strict consensus min = 12 steps, max = 14 steps. Evolution of this character (Fig. 7A) shows a pattern differing little from those of characters 1 and 2. Parsimony reconstructions indicate transverse veins sheathed by many layers of fibers evolved independently in Calamoideae, Coryphoideae, *Leopoldinia*, and within the clade of Attaleinae exclusive of *Jubaeopsis*. Both optimization methods indicate independent reversals back to sclerotic parenchyma occur in Caryoteae and *Phoenix* within Coryphoideae.

Transverse vein architecture in surface view (character 5; Fig. 7B; Appendices S6, S18): 0 = largest veins orthogonal, i.e., without abrupt change in angle; 1 = largest veins with irregular course, i.e., with abrupt change in angle. Two distinctive patterns of transverse vein architecture were found. In the first, the largest transverse veins are orientated more or less transversely and commonly connect with just major longitudinal veins (Fig. 4D, E, G, I–K). In the second pattern, transverse veins run obliquely between veins, especially smaller longitudinal veins, and form a zig-zag pattern (Fig. 4C, F, H).

Transverse vein architecture optimizes onto 95 trees with 13 steps, five trees with 14 steps; all changes within palms. State transitions within palms: 0→1 min = 5, max = 9; 1→0 min = 4, max = 9. Optimization onto strict consensus min = 12 steps, max = 14 steps. Although many deep nodes are reconstructed as equivocal, the distribution of states (Fig. 7B) shows a high degree of correspondence with those of characters 1, 2 and 4. ML reconstructions indicate that the sinuous, irregular transverse veins in Caryoteae evolved independently from those of Ceroxyloideae + Arecoideae. Orthogonally orientated transverse veins in Attaleinae evolved independently from those of Calamoideae and Coryphoideae.

Adaxial subepidermal fibers (character 6; Fig. 6B; Appendices S7, S19): 0 = absent; 1 = present as discontinuous to continuous fibers. Fibers replace parenchyma in hypodermal layer in some species (Figs. 2F, G; 3J, K).

Adaxial subepidermal fibers optimize onto 95 trees with 25 steps, five trees with 24 steps; all changes within palms. State transitions within palms: 0→1 min = 17, max = 25; 1→0 min = 0, max = 7. Optimization onto strict consensus min = 20 steps, max = 25 steps. With a similar pattern of evolution to character 3, adaxial subepidermal fibers have many independent gains throughout the family (Fig. 6B). Notably, parsimony optimizations

←

Thrinax, *Zombia*; [4] →1 *Kerriodoxa*; [5] →1 *Caryota ophiopelis*, *Arenga undulatifolia*; [6] →1 *Lodoicea*, *Borassodendron*; [7] →1 Livistoninae excluding *Livistona*; [8] →1 *Rhapis*; [9] →1 *Wendlandiella*; [10] →1 *Desmoncus*; [11] 1: *Acanthophoenix*, *Bentinckia*, *Calyptrocalyx*, *Cyrtostachys*, *Linospadix* + *Laccospadix*. (B) Adaxial subepidermal fibers optimizes onto 95 trees with 25 steps, five trees with 24 steps; all changes within palms. Superscript to right of a taxon denotes state change(s) within collapsed clades: [1] 0: *Hemithrinax* + *Leucothrinax*, *Thrinax*; [2] →1 *Borassodendron*; [3] →1 *Johannesteijsmannia*, *Pholidocarpus*, *Pritchadiopsis*; [4] →1 *Guihaia, Maxburretia* + *Rhapis*; [5] 0: all except *Ravenea* (1); [6] →1 *Wendlandiella*; [7] 0: all except *Asterogyne* (1); [8] 1: *Cyrtostachys*, *Loxococcus*, *Hydriastele*, *Marojejya darianii*; [a] 0: 21 trees, equivocal in 79 trees; [b] 1: 94 trees, eqivocal in six trees; [c] 0: 37 trees, equivocal in 63 trees.

reconstruct their presence in Calamoideae as a synapomorphy for the subfamily. A large proportion of the genera of Ceroxyloideae also have subepidermal fibers, though optimizations of this character are equivocal between the three tribes of the subfamily. Other notable gains occur at the basal node or within tribe Cryosophileae of Coryphoideae and several tribes within Arecoideae.

Nonvascular fiber bundles free in mesophyll (character 7; Fig. 8A; Appendices S8, S20): 0 = absent; 1 = present. Nonvascular fiber bundles may occur in the mesophyll without a connection to veins or surface layers (Fig. 2C, F, H, K).

The character nonvascular fiber bundles free in mesophyll optimizes onto 83 trees with 41 steps, 14 trees with 41 steps, three trees with 42 steps; all but two changes within palms. State transitions within palms: 0→1 min = 8, max = 15; 1→0 min = 24, max = 32. Optimization onto strict consensus min = 34 steps, max = 43 steps. Parsimony reconstructions of the evolution of nonvascular fibers indicate their presence as a plesiomorphic state within the family, with the majority of state transitions involving numerous losses (Fig. 8A). The loss of these fibers is optimized as a synapomorphy for Coryphoideae, *Pseudophoenix*, and several lineages of Arecoideae including Attaleinae.

Nonvascular fiber bundles attached to surface layer as a regularly repeating series (character 8; Fig. 8B; Appendices S9, S21): 0 = absent; 1 = present. Repeating series of fiber bundles occur in or adjacent to the adaxial hypodermis (Fig. 2D–G, J–L).

Nonvascular fiber bundles attached to surface layer(s) optimizes onto 86 trees with 32 steps, onto 14 trees with 31 steps; 28–30 steps within palms. State transitions within palms: 0→1 min = 3, max = 20; 1→0 min = 10, max = 26. Optimization onto strict consensus min = 22 steps, max = 35 steps. The presence of nonvascular fiber bundles attached to surface layers on one or both leaf surfaces is widely distributed among all subfamilies except for *Nypa* (Fig. 8B). All reconstructions demonstrate that the absence of this character within Coryphoideae and Ceroxyloideae represent losses. Arecoideae show substantial complexity in the evolution of this character.

Continuity of longitudinal veins with adaxial surface layers. This character can be scored in two ways, the first with two states (character 9a): 0 = bundle sheath extensions absent; 1 = veins bridged to surface layer by specialized bundle sheath extension cells. Bridges or buttresses of sclerenchyma join the veins to the adaxial surface layers (Fig. 2D–L) or bridges are absent (Fig. 2A–C).

The binary state version of this character optimizes onto all trees with 25 steps (not shown, see online Appendices S10 and S22). Optimizations show a general pattern to that described later.

Continuity of longitudinal veins with surface layers can also be scored for three states (character 9b; Fig. 9; online Appendices S11, S23): 0 = bundle sheath extension cells absent; 1 = veins bridged to adaxial surface layer by longitudinally elongate fibers; 2 = veins bridged to adaxial surface layer by vertically (ad/abaxially) elongate sclereids. Specialized bundle sheath extensions may consist of longitudinally elongated fibers (Fig. 2D, E, I–L) or a palisade of short, vertically elongate sclereids (Fig. 2F–H).

The multistate version of this character optimizes onto 99 trees with 25 steps, one tree with 24 steps; all but three changes within palms. State transitions within palms: 0→1 min = 5, max = 14; 0→2 min = 0, max = 5; 1→0 min = 2, max = 11; 1→2 min = 0, max = 0; 2→0 min = 1, max = 5; 2→1 min = 0, max = 1. Optimization onto strict consensus min = 23 steps, max = 25 steps. Ad/abaxial sclereids bridging the longitudinal veins to the adaxial surface layers characterize both Calamoideae and *Nypa* (Fig. 9). Vein-bridging cells in the form of longitudinally elongate fibers are restricted to the crown clade of palms exclusive of the latter two subfamilies. This type of bridging cell evolved independently in a minimum of four lineages: Coryphoideae, Ceroxyleae, *Iriratella* (Arecoideae), and Attaleinae.

Symmetry of lamina histology (character 10; Fig. 10; online Appendices S12, S24): 0 = dorsiventral; 1 = isobilateral. Overall symmetry of the lamina is defined by the arrangement of the mesophyll. A dorsiventral lamina has the palisade layer (if present) on the adaxial side and a looser layer on the abaxial side, usually with all or most of the stomates on the abaxial surface (Fig. 2A–D, F, K, L). An isobilateral lamina has palisade mesophyll on both ad- and abaxial sides and stomates on both surfaces in about equal density (Fig. 2E, I, J).

Symmetry of lamina histology optimizes onto 100 trees with 13 steps, 10 steps within palms. Parsimony state transitions within palms: 0→1 min = 6, max = 10; 1→0 min = 0, max = 4. Parsimony optimization onto strict consensus: min = 13 steps, max = 13 steps. Within this data set, state variation in lamina histology symmetry is restricted to Coryphoideae. Hence, Fig. 10 illustrates only this subfamily and details all genera studied within it. Parsimony reconstructions indicate that isobilateral lamina histology evolved independently in most genera possessing the state. The optimization of states at the node for *Sabal* + Cryosophileae (New World thatch palm clade) varies from dorsiventral to isobilateral depending on how generic relationships are resolved within Cryosophileae. Optimizations for trees that place *Trithrinax* sister to other Cryosophileae indicate isobilateral symmetry evolved at the basal node of the New World thatch palm clade. ML optimizations at this node are always equivocal. Within Borasseae, parsimony optimizations are equivocal for most nodes. ML optimizations, however, indicate isobilateral symmetry is the ancestral state for Borasseae, with dorsiventral symmetry independently gained in each of the three genera showing this state.

Tests of phylogenetic independence—Correlation analysis does not show strong support across all trees for rejecting the hypothesis of phylogenetic independence for any of the nine anatomical characters with respect to leaf type (Table 1). Of the 36 pairwise comparisons between the nine anatomical

→

Fig. 7. Summary of parsimony reconstructions of ancestral states for 100 trees displayed onto strict consensus for (A) transverse vein sheath cell type and (B) transverse vein architecture. Summary of maximum likelihood reconstructions indicated in circles below branches that differ from parsimony results. (A) Transverse vein sheath cell type optimizes onto 100 trees with 14 steps, 12 within palms. Superscript to left of a taxon denotes state change(s) within collapsed clades: [1] 1: *Coccothrinax*, *Cryosophila*, *Schippia*; [2] →1 *Hyphaene* + *Medemia*; [3] →1 *Chamaerops*. (B) Transverse vein architecture optimizes onto 95 trees with 13 steps, five trees with 14 steps; all changes within palms. Superscript to right of a taxon denotes state change(s) within collapsed clades: [1] 0: *Chelyocarpus*, *Hemithrinax*, *Itaya*; [2] →1 *Hyphaene* + *Medemia*; [3] →0 *Maxburretia*.

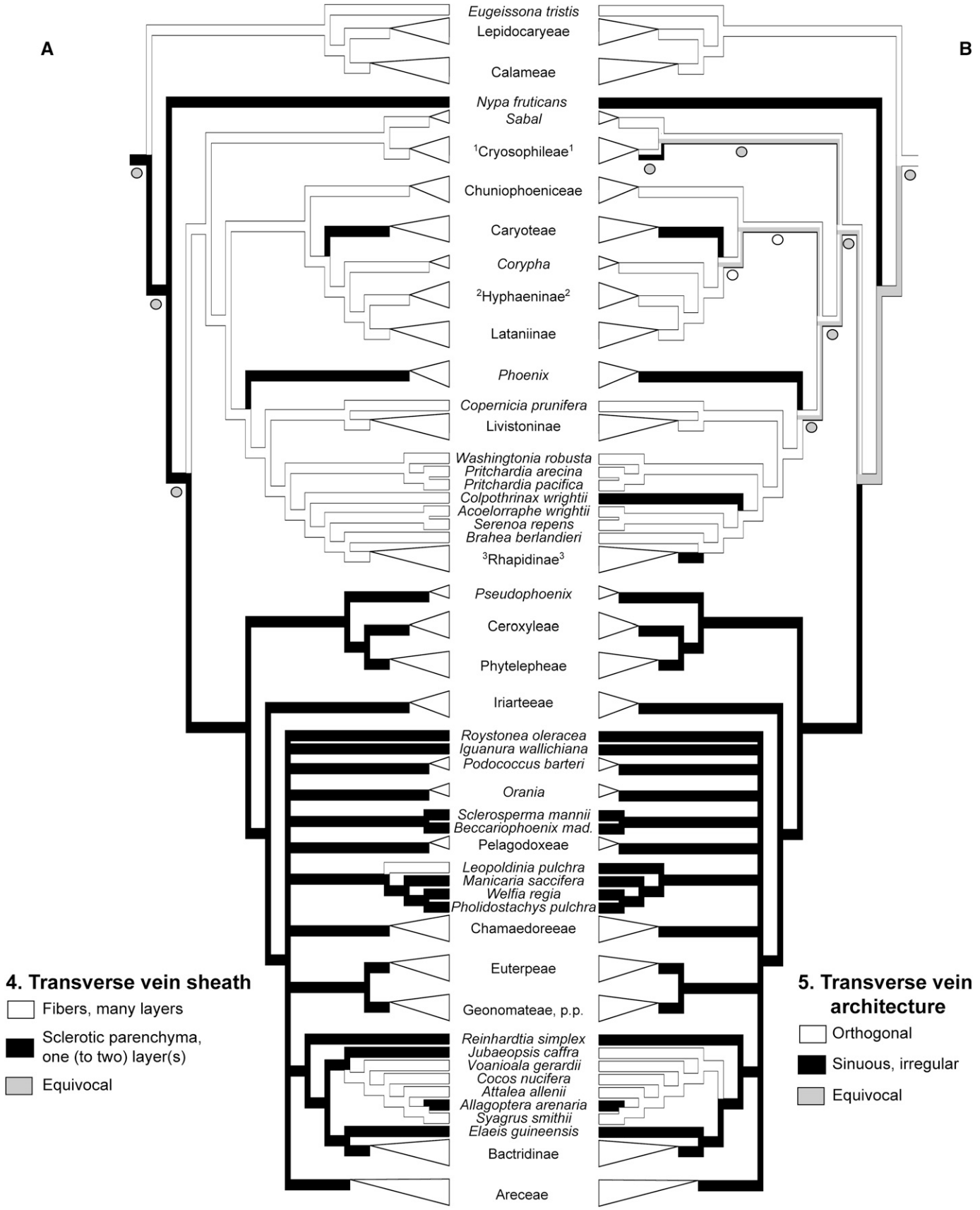
A
B
Eugeissona tristis
Lepidocaryeae
Calameae
Nypa fruticans
Sabal
[1]Cryosophileae[1]
Chuniophoeniceae
Caryoteae
Corypha
[2]Hyphaeninae[2]
Lataniinae
Phoenix
Copernicia prunifera
Livistoninae
Washingtonia robusta
Pritchardia arecina
Pritchardia pacifica
Colpothrinax wrightii
Acoelorraphe wrightii
Serenoa repens
Brahea berlandieri
[3]Rhapidinae[3]
Pseudophoenix
Ceroxyleae
Phytelepheae
Iriarteeae
Roystonea oleracea
Iguanura wallichiana
Pododoccus barteri
Orania
Sclerosperma mannii
Beccariophoenix mad.
Pelagodoxeae
Leopoldinia pulchra
Manicaria saccifera
Welfia regia
Pholidostachys pulchra
Chamaedoreeae
Euterpeae
Geonomateae, p.p.
Reinhardtia simplex
Jubaeopsis caffra
Voanioala gerardii
Cocos nucifera
Attalea allenii
Allagoptera arenaria
Syagrus smithii
Elaeis guineensis
Bactridinae
Areceae
4. Transverse vein sheath
Fibers, many layers
Sclerotic parenchyma, one (to two) layer(s)
Equivocal
5. Transverse vein architecture
Orthogonal
Sinuous, irregular
Equivocal

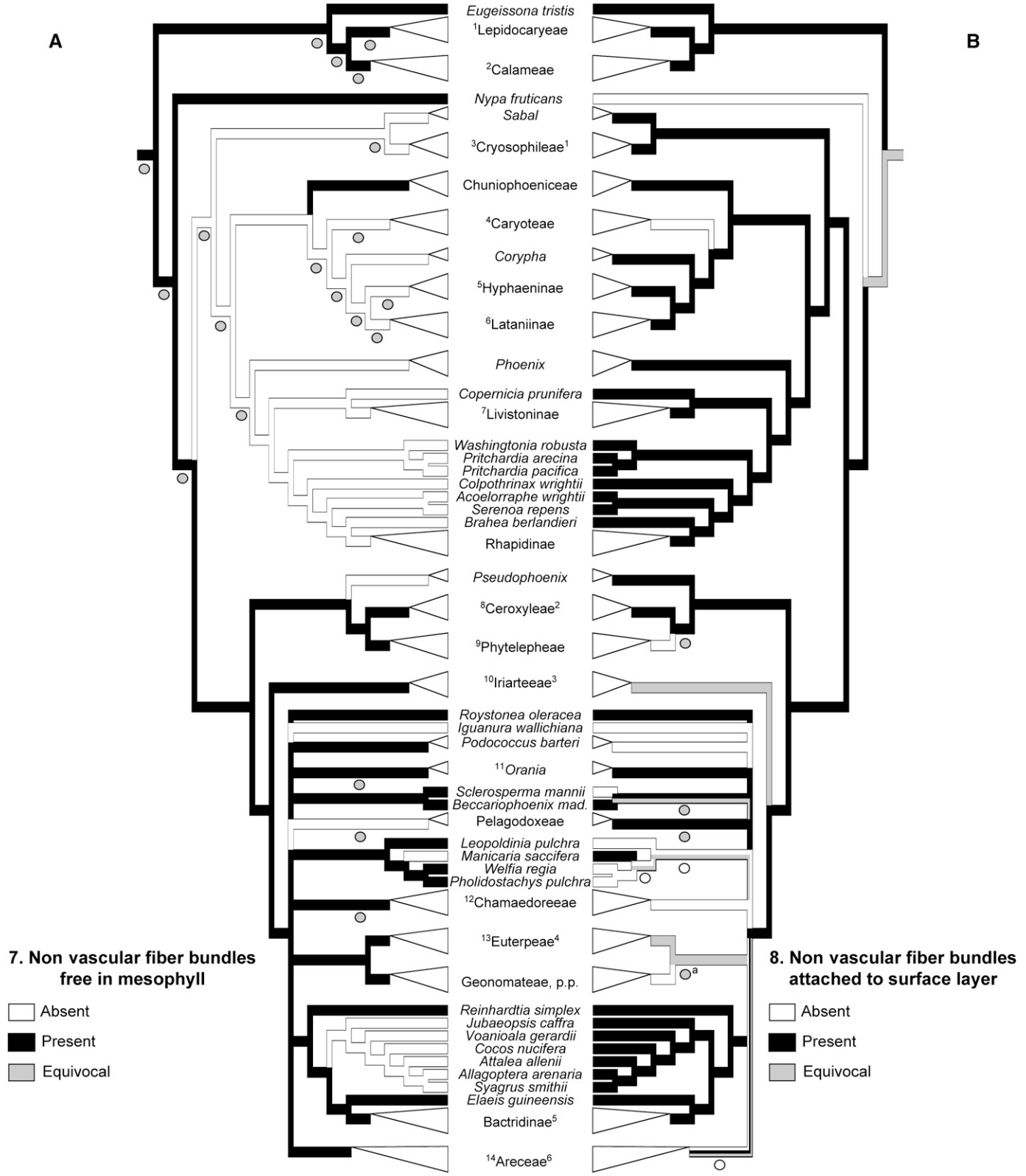

Fig. 8. Summary of parsimony reconstructions of ancestral states for 100 trees displayed onto strict consensus for (A) nonvascular fiber bundles free in mesophyll and (B) nonvascular fiber bundles attached to surface layer. Summary of maximum likelihood reconstructions indicated in circles below branches that differ from parsimony results. (A) Nonvascular fiber bundles free in mesophyll optimizes onto 83 trees with 41 steps, 14 trees with 41 steps, three trees with 42 steps; all but two changes within palms. Superscript to left of a taxon denotes state change(s) within collapsed clades: [1] →0 *Eremospatha* + *Laccosperma*, *Mauritia*; [2] →0 *Korthalsia*, *Pigafetta*, *Plectocomia*; [3] 1: *Hemithrinax*, *Zombia*; [4] 1: *Arenga hookeriana*, *Wallichia*; [5] →1 *Hyphaene* + *Medemia*; [6] →1 *Latania*; [7] →1 *Johannesteijsmannia* + *Pholidocarpus*; [8] →0 *Juania*; [9] →0 *Ammandra*; [10] →0 *Socratea*; [11] →0 *Orania*

characters, 14 are significant at the $P < 0.01$ threshold across all trees, indicating strong support for the hypothesis of correlated evolution. Five of these significant results inform correlations among the surface layers (cell shape in surface view of epidermis and hypodermis, Fig. 5) and the network of transverse veins (sheath cell type and architecture, Fig. 7). The presence or absence of a regularly repeating series of nonvascular fiber bundles in contact with the surface layers significantly correlates with each of the four characters just described as well as the presence or absence of both nonvascular fiber bundles free in the mesophyll and cells that bridge longitudinal veins to at least one surface layer. Contour of the anticlinal walls of the epidermal cells shows significant correlations with both hypodermal cell shape and the presence or absence of subepidermal fibers. The occurrence of subepidermal fibers also significantly correlates with transverse vein architecture.

DISCUSSION

Homoplasy—Although the evolution of all nine major anatomical characters (plus symmetry of lamina histology) is highly homoplasious, reconstruction of ancestral states for each character demonstrates that many clades recognized within the palm family (Dransfield et al., 2005, 2008b) are characterized by independent, unambiguous transitions to an apomorphic state. In fact, a large proportion of the homoplasious evolution observed in most characters occurs among major groups within palms, as opposed to being a phenomenon mainly restricted to terminal lineages. While state assignment to the basal node of palms and the two deepest nodes within the crown clade exclusive of Calamoideae is equivocal for many parsimony reconstructions and nearly all likelihood reconstructions, character state assignment to each of the basal subfamilial nodes is usually unambiguous under both methods. As likelihood reconstructions take into account branch lengths, so as to modulate the probability of state transformations accordingly, our results obtained for the basal nodes within palms are within expectation, given the relatively very long branch between palms and the outgroup taxa and those within the outgroups (Cunningham et al., 1998). Sannier et al. (2007), in an investigation of evolution of palm pollen microsporogenesis and using a subset of the phylogenetic data employed in this study, obtained similar likelihood reconstructions for these early nodes within palms despite uniform state codings for the outgroups Calamoideae and Nypoideae.

The significant macroevolutionary patterns that emerge from our analyses need further discussion. Because we conducted ancestral state reconstructions and tests of phylogenetic independence over a set of 100 trees that collectively account for nearly all topological conflict present in the results of Asmussen et al. (2006), they reflect in parallel a conservative view of what can and cannot be inferred about the evolution of palms. The recurrence of similar character states is not random with respect to phylogeny among the nine leaf anatomical characters examined. Significant correlations do exist, as evinced by both inspection of the ancestral state reconstructions and the results of pairwise tests of phylogenetic independence. Because we chose these characters based on of their perceived biological significance, the synthesis of our results suggests the repeated evolution of different suites of anatomical character states as alternative functional units.

Anatomy and morphology of palm leaves—Surprisingly, there is no clearly palmate or pinnate type of leaf anatomy even though leaf morphological type is perhaps the most readily perceptible point of differentiation among palms. Lamina anatomy is not strongly correlated with leaf type across any of the nine characters tested (Table 1), an inference that can be extended to other anatomical characters (Tomlinson, 1961). Although this finding could be interpreted as a consequence of categorical oversimplification (palmate leaves of Coryphoideae show appreciable variability in form) (Dransfield et al., 1990), ancestral state reconstructions indicate phylogenetic contingency better explains this result. Thus the three genera of fan palms in Calamoideae (Lepidocaryeae: Mauritiinae; Fig. 1) share the unique suite of character states that distinguish the subfamily (Figs. 5A, B; 6A, B; 7A, B; 8B; 9; see also Tomlinson, 1961). Likewise, the anatomy of the pinnately compound coryphoid *Phoenix* (date palms) is similar to that of many genera of its palmate-leaved sister clade (Trachycarpeae), especially *Copernicia*. Shared anatomical features between the pinnate to bipinnate Caryoteae (Coryphoideae) and members of the Ceroxyloideae + Arecoideae clade (pinnate), as well as those between members of the latter clade and coryphoid fan palms, are discussed later.

The correlation between leaf type and venation architecture, highly significant across just part of its range (Table 1), warrants comment. All calamoid and many coryphoid genera with palmate leaves have a venation architecture that consists of transverse veins approximately orthogonal (perpendicular) to longitudinal veins, and which are often sheathed by many layers of fibers. Although the lengths of these veins vary within an individual leaf, in many genera the course of the largest of these veins spans the distance between adjacent ribs (or from midrib to lamina margin in the divided portion of the blade). Sack et al. (2008) suggest that such a network of venation, providing a high degree of vascular redundancy, confers tolerance to hydraulic disruption. From a biomechanical perspective, well-developed transverse veins in palmate leaves can function as stringers between the ribs, so sustaining lateral loading forces, as hypothesized by Niklas (1992, 1999). Such venation, however, also has a wide distribution among pinnate taxa because it is prevalent in the remaining Calamoideae and also frequent in subtribe Attaleinae (Arecoideae: Cocoseae). This is discussed in detail later.

Although not included in our analyses, the relationship between lamina anatomy and lamina size is of inherent interest.

←

ravaka (*trispatha*); [12] →0 *Chamaedorea* + *Gaussia*, *Hyophorbe*; [13] →0 *Euterpe*; [14] 0: *Areca* + *Nenga*, *Bentinckia*, *Carpentaria* + *Wodyetia*, *Carpoxylon*, *Clinosperma*, *Clinostigma*, *Cyphophoenix*, *Cyrtostachys*, *Dictyosperma*, *Lavoixia* + *Brongniartikentia*, *Phoenicophorium*, *Ptychosperma*, *Rhopaloblaste*, *Roscheria*, *Veitchia*. (B) Nonvascular fiber bundles attached to surface layer(s) character optimizes onto 86 trees with 32 steps, onto 14 trees with 31 steps; 28–30 steps within palms. Superscript to right of a taxon denotes state change(s) within collapsed clades: [1] 0: *Chelyocarpus*, *Itaya*; [2] →0 *Ravenea*; [3] 1: *Dictyocaryum*, *Iriartella*; [4] 0: *Euterpe*; [5] 0: *Aiphanes*, *Bactris*; [6] 1: *Actinorrhytis*, *Bentinckia*, *Campecarpus*, *Carpoxylon*, *Clinostigma*, *Cyphophoenix*, *Cyphosperma*, *Cyrtostachys*, *Dictyosperma*, *Hydriastele*, *Loxococcus*, *Marojejya darianii*, *Rhopaloblaste*; [a] 0: 37 trees, equivocal in 63 trees.

The enormous range in absolute leaf size that palms display is the largest of any angiosperm family, from less than 0.5 m long in some species of *Chamaedorea* (Hodel, 1992) and *Dypsis* (Dransfield and Beentje, 1995) to a record 25.11 m in *Raphia regalis* Becc. (Calamoideae; Hallé, 1977). These pinnate taxa mark the endpoints of length range, but palmate-leaved taxa are about as impressive—the giant talipot palm, *Corypha umbraculifera* L. has leaves up to 8 m wide (Tomlinson, 2006). For leaves of such great adult size, there is a comparable great range within the individual plant, which starts with small juvenile leaves, a consequence of establishment growth. The anatomy of both these champion leaves includes a high volume fraction of sclerenchyma distributed in multiple ways in each (Figs. 6B; 7A; 8A, B; 9), in addition to a well-developed network of long transverse veins (Fig. 7B). These histological features can provide ample mechanical reinforcement. In contrast, other impressively large palm leaves, such as those of some *Arenga* species (Coryphoideae: Caryoteae; to 8.5 m) and *Welfia regia* (Arecoideae; to 6 m; Henderson et al., 1995), have little evident internal structural support. Very different leaf anatomical configurations, as evinced by our character data, are therefore capable of sustaining these giant leaves. We provide a possible explanation for this apparent paradox below (see *Evolution of the surface layers*).

If qualitative character data have an unclear relationship with leaf size, then our observations suggest anatomy does have a quantitative relationship with size. The leaf axis (petiole; also rachis of pinnate leaves) and ribs associated with plications in the leaf show this relationship most clearly. Congruent with mechanical principles, the cross-sectional area of these structures scales positively with leaf size. However, the relative proportion of vascular bundles to ground tissue remains relatively invariant. In potential compensation, the proportion of lignified tissue, as seen in both in the volume fraction of vascular fibers (i.e., sheath thickness) and in the extent of lignification of ground tissues, also appears to scale positively with size. Lamina thickness has an imprecise relationship with leaf size. In a survey of this trait across all genera of the family, the thickest leaves we measured were mostly from taxa occurring in somewhat seasonally arid climates (J. W. Horn, unpublished data).

Evolution of the surface layers—The surface layers of the palm lamina—epidermis and hypodermis—evolve in close tandem and appear to function as a unit, comprising the "rind" or mechanical skin of the leaf, when modeled on engineering principles (Gibson et al., 1988; Niklas, 1999; Meicenheimer et al., 2008). The capability of these two compartments to function in concert across the whole of Arecaceae is suggested by our experience in making surface preparations of the epidermis. The palm epidermis does not peel, it must be scraped (Tomlinson, 1961), and in doing so, the hypodermis cannot be disconnected from the epidermis. Bonding between these layers is comparatively much stronger than between other tissues of the lamina.

As differing cell geometries can strongly affect the mechanical behavior of cellular solids (Niklas, 1992; Gibson and Ashby, 1997), significantly correlated evolution in epidermal and hypodermal cell shape in surface view suggest a functional significance to this pattern. Although the difference between quadrangular and hexangular epidermal and hypodermal cells may initially seem slight, palm epidermal and hypodermal cells, aside from those associated with stomata and trichomes, are typically anisotropically extended. Cells with a hexagonal outline may be extended in three planes, while quadrangular cells are extended in a linear direction. Thus, combinatorial possibilities are maximized when hexagonal cells with varying inclination are present in both the epidermis and hypodermis. In palm leaves with surface layers of hexagonal cells, hypodermal cells are most often transversely extended, whereas the epidermal cells are extended in another diagonal plane, giving the cell a "spindle-shaped" outline and tending to obscure longitudinal files of cells. The angle of incidence between the elongated anticlinal cell walls of these two layers is therefore strongly oblique to nearly perpendicular, creating a cross-laminated network of plies. Similar to plywood in this regard (Giraud-Guille, 1998), the cross-laminated surface layer type likely shows many corresponding mechanical properties. Relative to other palm surface layer types, which are parallel-laminated, cross-laminated surface layers should show both equalized in-plane strength and overall increased load-bearing capacity normal to the lamina surface, assuming other factors are equal. Substantially larger forces would be required to induce face yield and buckling (Gibson and Ashby, 1997). Surface layers similar to the cross-laminated type in palms occur in *Heliconia*, to which Rundel et al. (1998) attribute a mechanical role in lamina support, enabling the large blades of many species to remain functionally intact subsequent to their segmentation by wind or other external disturbances.

Nypa, tribe Caryoteae (Coryphoideae), and Arecoideae evolved the cross-laminated surface layer type in parallel; notable losses within Arecoideae occur in Areceae, Euterpeae, and subtribe Attaleinae of Cocoseae (Fig. 5). *Nypa*, the mangrove palm, shows fundamental differences from the other taxa because its epidermal cells are quite regularly hexagonal and its hypodermal cells are unusual among all palms in being thick-walled and lignified. The biomechanical hypothesis discussed is supported by correlations between Caryoteae (Coryphoideae) and those Arecoideae that both possess the cross-laminated surface layer type. Among all palms, these lineages have the correspondingly lowest proportion of mechanical tissue in their laminae. The low volume fraction of mechanical tissue in Arecoideae may be explained by both phylogenetic contingency with a subsequent correlated loss of fiber bundles in contact with the surface layers. However, the loss of mechanical tissue from Caryoteae is remarkable within their phylogenetic context because they are embedded within a clade that otherwise exemplifies the deployment of abundant fibers for structural support. Because lignin synthesis requires a high resource investment (Chabot and Hicks, 1982; Chapin, 1989; Niklas, 1997), the evolution of a mechanically strong lamina surface layer that reduces the need for a high volume fraction of lignified tissues for structural support may be hypothesized as a design optimum within palms. A reduced volume fraction of fibers within the lamina has the additional potential benefit of increasing the relative mass fraction of chlorenchymatous mesophyll tissue, which is associated with higher mass-based photosynthetic rates (Garnier et al., 1999; Niinemets et al., 2007). Although the species-richness of Caryoteae is about equal to that of its sister clade (*Corypha* + Borasseae), the evolution of the cross-laminated surface layer type within Arecoideae deserves further investigation as one of a combination of structural traits that enabled the prominent diversification of this clade.

In addition to cell shape, the contour of the anticlinal walls of the epidermal cells is of perceived biomechanical significance. Tomlinson (1990) and Niklas (1992) suggest that sinuous cell walls allow adjacent cells to interlock like pieces in a jigsaw puzzle and should increase the mechanical strength of the

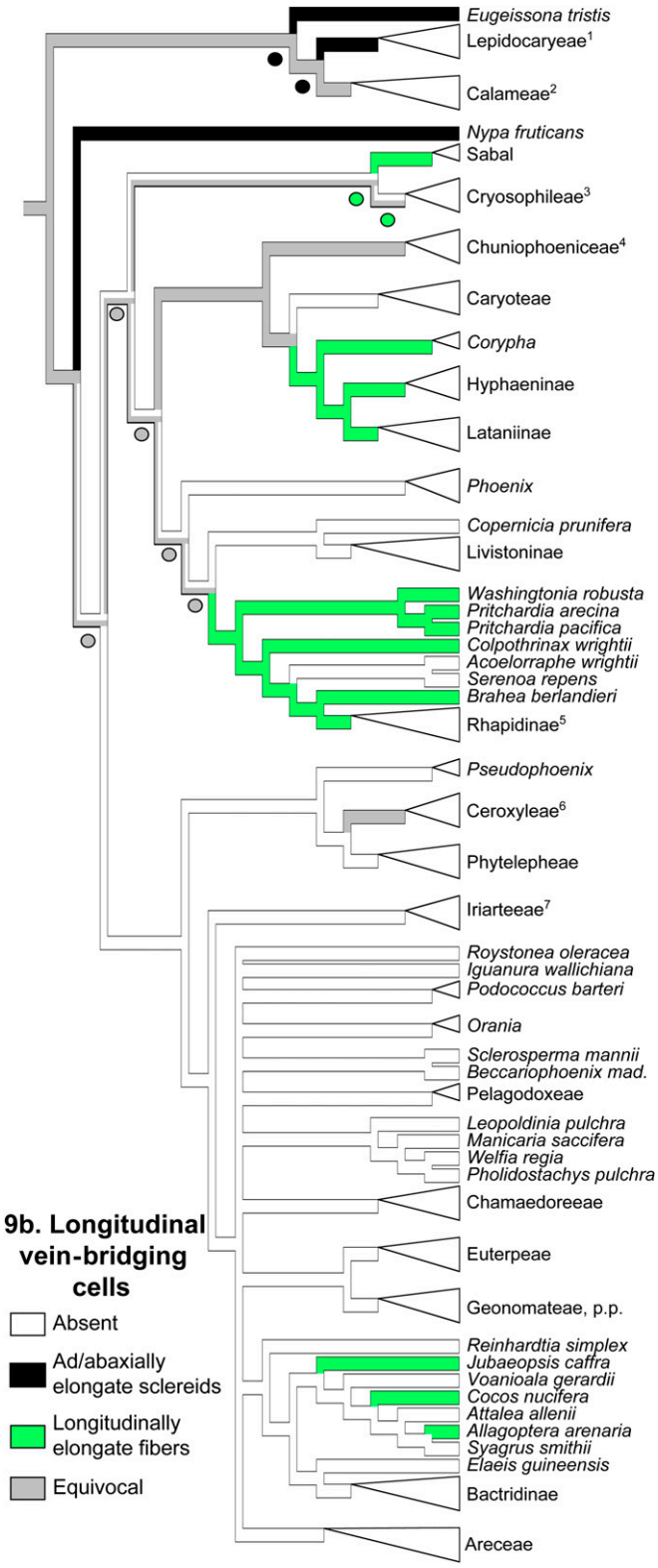

Fig. 9. Summary of parsimony reconstructions of ancestral states for 100 trees displayed onto strict consensus for character 9b. Longitudinal vein-bridging cells (multistate version). Character optimizes onto 99 trees with 25 steps, one tree with 24 steps; all but three changes within palms. Summary of maximum likelihood (ML) reconstructions indicated in circles below branches that differ from parsimony results. Superscript denotes state change(s) within collapsed clades: [1] →0, *Laccosperma*; [2] 1: *Metroxylon*+*Plectocomia*, *Pigafetta*; [3] 0: *Chelyocarpus*, *Itaya*, *Thrinax*; [4] 2: *Chuniophoenix*, *Nannorrhops*; [5] →0 *Guihaia*, *Rhapis*; [6] 2: *Ceroxylon*+*Juania*, *Oraniopsis*; [7] →2, *Iriartella*. Character 9a, a binary state version of this character optimizes onto all trees with 25 steps (online Appendices S11, S23). Parsimony reconstructions here infer no differences in state assignment to nodes with regard to the presence or absence of bridging cells (regardless of type). ML reconstructions over 100 trees all assign the presence of bridging cells (state 1) to the basal and all internal, equivocal nodes of Coryphoideae for the tree shown, excepting the basal node of Trachycarpeae and *Phoenix*+Trachycarpeae (equivocal).

epidermal layer. Likewise, fibers adjacent to the epidermis may contribute substantially to the rigidity and strength of leaves, as shown by Vincent (1982) for the grass *Lolium perenne*. Both of the above character states show a wide but scattered distribution among palms, but nevertheless evolved in a significantly parallel association (Fig. 6; Table 1). As such, the correlation may be interpreted as a variant optimum in the construction of the surface layer "skin" of the lamina. The efficacy of the mechanical characteristics of this surface layer type supported by its commercial use as raffia, an early raw material used for making cordage and textiles, which is produced from the adaxial surface layers of the leaf lamina of the calamoid *Raphia farinifera* (Tomlinson, 1961; Sandy and Bacon, 2001). Mechanical tests show it to have similar properties to many natural fibers of commercial value (Sandy and Bacon, 2001). Further corroborating this hypothesis is that the evolution of sinuous anticlinal cell walls is significantly correlated with rectangular hypodermal cells, hence, not associated with cross-laminated surface layer type. Notable lineages that possess a sinuous surface layer type are Calamoideae, Coryphoideae (subtribe Livistoninae and Trachycarpeae), and in Arecoideae tribes Cocoseae (within subtribe Attaleinae), Euterpeae, and Pelagodoxeae.

Evolution of the venation network of the lamina—Critical to the mechanical stability of all but the smallest leaves of terrestrial plants is a network of strong, usually lignified cells that provide the scaffolding or internal skeleton around which other leaf tissues are organized (Lucas et al., 1991; Choong et al., 1992; Niklas, 1999; Roth-Nebelsick et al., 2001) In palms and many other monocots, this network not only consists of veins but includes nonvascular fibers that, at least in palms, usually occur grouped in bundles that are either positioned in contact with the surface layers, or else may be independent of the surfaces and "free" in the mesophyll. The longitudinal veins of some palms have fibers or sclereids that effectively attach the vein along the length of its course to one or both surface layers. Thus functioning much like an I- or T-beam, these cells reinforce the leaf via both material and, collectively, structural properties (Schwendener, 1874; Read and Stokes, 2006). An unresolved observation is the presence of fibers that ramify freely in the lamina in genera belonging to three different subfamilies (Tomlinson, 1961). Tomlinson and Fisher (2005) suggest that similar fibers in *Gnetum* leaves have a role in effecting hydration of the lamina in addition to mechanical support.

Transverse veins—Within the venation network of palms, the architecture of the transverse veins and the form of their sheath cells vary considerably. Transverse veins have two fundamentally different architectural arrangements (Fig. 4): first, a course that is approximately orthogonal to the longitudinal veins, the

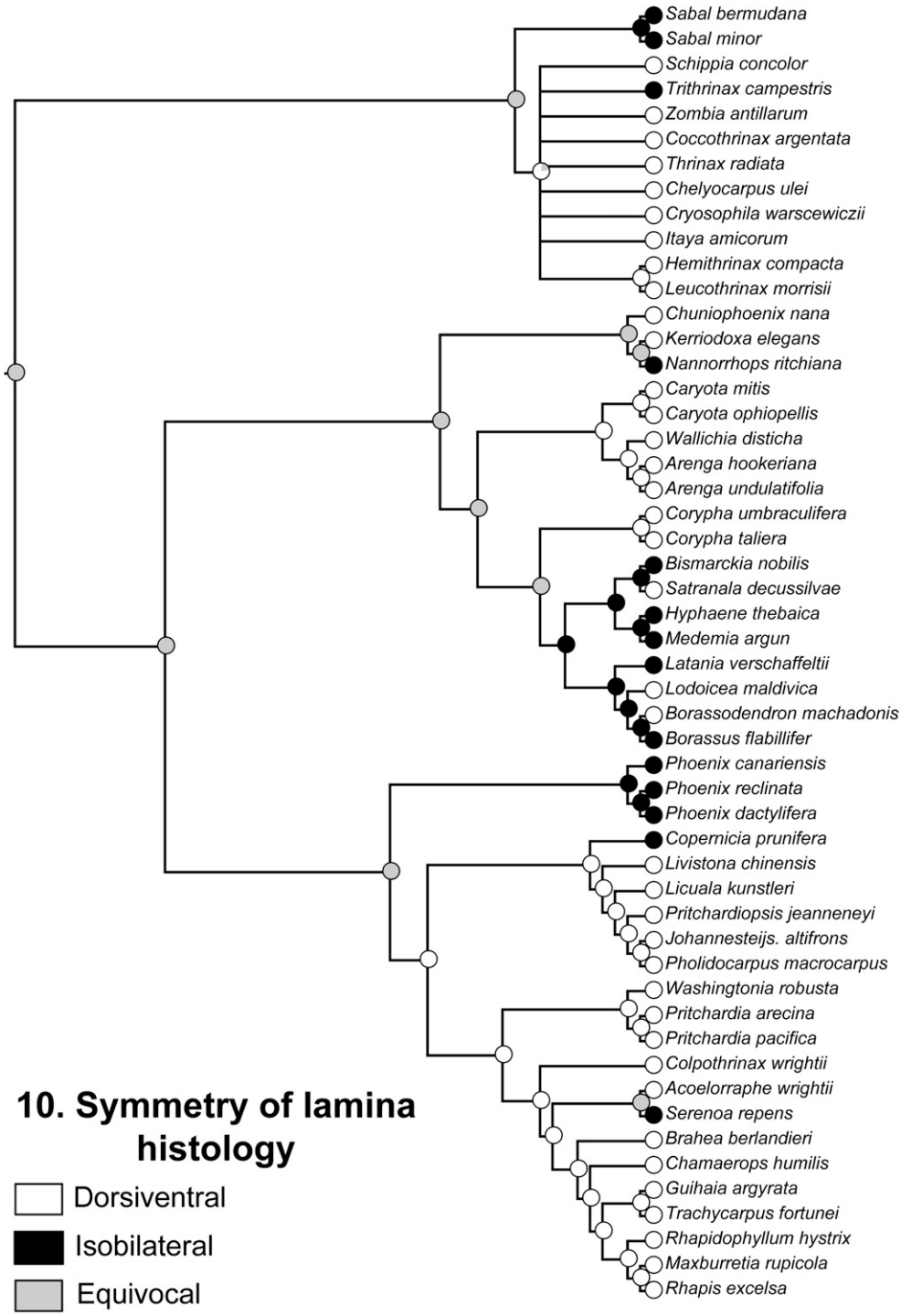

Fig. 10. Evolution of symmetry of lamina histology in subfamily Coryphoideae. Tree shown pruned at basal node of subfamily from full analysis; no nodes collapsed. Within this data set, state variation in lamina symmetry is restricted to this subfamily. *Butia* (Arecoideae: Cocoseae: Attaleinae; not sampled) alone represents the single gain of this state outside Coryphoideae. Summary of maximum likelihood optimizations for 100 trees onto the strict consensus of these trees. Parsimony reconstructions for 100 trees each optimize with 13 steps, 10 steps within palms.

longest of these veins often extending laterally in the lamina and not connecting with many longitudinal veins (Fig. 4D, E, G, K); and second, a course that is highly sinuous and irregular, the veins usually short and connecting frequently with longitudinal veins (Fig. 4H–J). Parallel evolution between architecture and sheath cell type is also evident (Fig. 7). Orthogonal transverse veins sheathed by many layers of thick-walled fibers occur in Calamoideae, many Coryphoideae, and are clearly independently derived within Attaleinae. Sinuous transverse veins sheathed by sclerotic parenchyma evolved many times, as

TABLE 1. Pairwise tests of correlated evolution between leaf type (pinnate vs. palmate) and nine major anatomical characters. Range of log likelihood test statistics ($-2\ln L$) reported for 100 trees. Anatomical characters: 1, adaxial epidermal cell shape; 2, adaxial hypodermal cell shape outline; 3, adaxial epidermal cell anticlinal wall contour; 4, transverse vein sheath cell type; 5, transverse vein architecture; 6, adaxial subepidermal fibers; 7, nonvascular fiber bundles free in mesophyll; 8, nonvascular fiber bundles attached to surface layer; 9a, longitudinal veins attached to surface layers. Significance was assessed in context of χ^2 distribution with four degrees of freedom; ns = $P > 0.05$, * = $P < 0.05$, ** = $P < 0.01$, *** = $P < 0.001$. Boldface entries are those with strong significance over the entire range of test statistics for 100 trees.

		Anatomical character							
Anatomical character	Leaf type	1	2	3	4	5	6	7	8
1	11.2864*– 13.4601**								
2	4.2007 ns– 6.3429 ns	**21.2991*****– **21.9686*****							
3	3.5358 ns– 7.5417 ns	8.1144 ns– 22.1667***	**20.1896*****– **24.9586*****						
4	10.9655*– 17.1917**	**20.0916*****– **21.9243*****	7.6925 ns– 7.8541 ns	0.0248 ns– 13.7118**					
5	2.1315 ns– 23.3127***	**27.1933*****– **29.6000*****	**15.7148****– **16.6554****	0.5743 ns– 13.315**	**26.5351*****– **53.7411*****				
6	4.5892 ns– 5.1852 ns	12.4307*– 17.8131**	8.1519 ns– 41.1677***	**19.4373*****– **40.6685*****	3.2802 ns– 3.9518 ns	**14.6736****– **17.6433****			
7	1.4430 ns– 6.3285 ns	5.6507 ns– 6.4937 ns	2.6162 ns– 3.0084 ns	9.0709 ns– 9.4176 ns	6.0467 ns– 6.6843 ns	5.0067 ns– 9.6955*	1.7111 ns– 1.8993 ns		
8	7.0771 ns– 9.5284*	**25.9320*****– **29.6681*****	**13.3575****– **18.0113****	6.3005 ns– 10.3770*	**15.8318****– **20.3917*****	**16.2286****– **22.9455*****	4.9005 ns– 11.7228*	**14.7195****– **16.4744****	
9a	0.2487 ns– 8.9658 ns	2.8951 ns– 10.34949*	6.1557 ns– 9.6288*	1.6310 ns– 5.0639 ns	12.6089*– 13.5589**	12.9786*– 26.3816***	2.0225 ns– 7.4176 ns	1.3146 ns– 1.6814 ns	**17.1602****– **26.8608*****

in *Nypa*, Caryoteae, *Hyphaene* + *Medemia*, *Phoenix*, and the clade of Ceroxyloideae + Arecoideae (exclusive of Attaleinae). Although the relationship between venation architecture and sheath cell type is not absolute—several palmate-leaved genera of Coryphoideae have fiber-sheathed veins that are sinuous (Fig. 4C)—it is the most significant of the correlations we tested (Table 1). Because all palm leaves are fundamentally plicated structures, the positioning of a transversely orientated series of mechanically strong veins is congruent with physical principles; they reinforce the palmate lamina or pinnate pinna against bending forces that develop over the second moment of area (Niklas, 1992). The mechanically weaker sinuous veins have largely evolved in parallel with the cross-laminated surface layer type. Tests of correlated evolution are highly significant for three of the four pairwise combinations between these characters. Taken together, these results further corroborate the hypothesis of biomechanical significance of the cross-laminated surface layer type, as again, the investment in mechanical tissue in the venation network here decreases significantly. The relationship between the volume fraction of lignified leaf tissue and leaf longevity in palms deserves exploration. Studies indicate that leaf mass per area is positively correlated with leaf lifespan, which in turn is linked to growth rate (Wright and Westoby, 2002; Wright et al., 2004). Thus, beyond mechanics, these major differences in lamina construction may correspond to basic differences in growth strategy.

Longitudinal veins and fibers—Nonvascular fiber bundles of both types of distribution (surface vs. mesophyll) are common throughout palms and co-occur in many taxa. These two characters have an evolutionary pattern in which losses of fiber bundles free in the mesophyll are concentrated among lineages that possess fiber bundles in contact with surface layers (Fig. 8). Indeed this is the only highly significant correlation between mesophyll fibers and any of the other characters tested (Table 1). While fiber bundles associated with the surface layers are of strong mechanical significance, (Schwendener, 1874; Vincent, 1982, 1991), unlignified mesophyll fiber bundles may possibly also effect hydration of the mesophyll because they are either not or only weakly lignified (Tomlinson and Fisher, 2005). The parallel loss of these fiber bundles in the major palm lineages associated with arid climates suggests this.

Among the key strategies for structural support present within the possible range of variation in palm lamina anatomy is the occurrence of sclerenchyma cells juxtaposed between the longitudinal veins and one or both surface layers. These cells, by bridging internal and superficial zones of the lamina, stiffen the lamina to an extent, possibly minimizing reliance on hydrostatic support by mesophyll cells. Our results indicate that "bridging" of the veins to the surface layers is effected in two ways within palms. Calamoideae and *Nypa* differ from other palms in possessing *vertically elongate*, *cylindrical sclereids* that form a longitudinal palisade between the adaxial side of a vein and the adaxial surface layers. The clade of palms containing the other three subfamilies form vein to surface layer connections with *longitudinally elongate fibers*. The evolution of vein bridging by longitudinally elongate fibers has evolved independently in a minimum of four lineages within the clades: Coryphoideae, Ceroxyleae, *Iriartella*, and Attaleinae (Fig. 9). In these lineages, we suggest that the bridging connection was established through synorganization between veins and superficial nonvascular fiber bundles because these two characters have a parallel phylogenetic pattern. Moreover, they significantly correlate with each other and have a clear topographic relationship within the leaf.

Groups of cells that bridge veins to the surface layers, frequently referred to as bundle sheath extensions, occur in many angiosperm families (Wylie, 1952; Kenzo et al., 2007), and characterize a functional class termed heterobaric leaves

(Terashima, 1992; Nikolopoulos et al., 2002; Kenzo et al., 2007; Leegood, 2008) on account of their strong partitioning effect on whole-leaf physiology (Mott and Buckley, 2000). Heterobaric leaves are known to confer a range of potentially adaptive benefits relating to growth in seasonally arid and/ or cold climates. These include structural support under water stress (Kenzo et al., 2007), patchy stomatal behavior, with attendant accelerated stomatal response to drought (Terashima, 1992), and the channeling of light within the mesophyll of thick leaves to maximize photosynthetic rate (Karabourniotis et al., 2000; Nikolopoulos et al., 2002).

These observations support our idea that the evolution of vein-bridging cells—particularly in the form of fibers—may have been a key innovation that allowed palms to occupy arid or cold climates. Phylogenetic data allow the interpretation of extratropical adaptation as a series of few, historically independent events that closely coincide with the lineages mentioned that have fiber bridges. Major exceptions to this correspondence are few. For example, *Iriartella*, which occurs in wet tropical forests (Henderson, 1990), has a narrow fiber bridge only a single cell wide. *Pseudophoenix,* indigenous to seasonally dry areas of the Caribbean, is difficult to interpret on account of its unusual anatomy relative to other palms because it includes a continuous fibrous hypodermis many layers deep and is without bridged veins (Tomlinson, 1961; Read, 1968).

The radiations into drier and/or colder climates, though not promoting speciation to a degree seen in some wet tropical lineages (e.g., *Calamus*, *Licuala*, Areceae), are nevertheless important facets of palm macroevolution because many are characterized by an unusually high degree of structural novelty. Outstanding examples of this phenomenon occur in Coryphoideae, where *Hyphaene* and *Nannorrhops* (indigenous to regions with strongly arid climates) have unusual architectural innovations that include among the few instances of dichotomous aerial branching in palms (Hallé et al., 1978). The recently discovered genus *Tahina*, a narrow endemic of semiarid northwestern Madagascar, also exemplifies this phenomenon. *Tahina* is characterized by such an unusual mosaic of structural traits (including a massive, terminal inflorescence), present among genera of several related tribes, that it bears little resemblance to its sister genus, *Kerriodoxa*, except in a few technical details (Dransfield et al., 2008a). Radiations into dry habitats are also important because they include many species that are distinctive and dominant components of the vegetation types in which they occur. Familiar examples include many species of *Sabal* in the seasonally dry Caribbean Basin (Zona, 1990), as well as several species of *Borassus* that thrive in drier tropical regions of Africa and Southeast Asia (Bayton, 2007).

Convergent evolution of lamina anatomy within palms—Our analyses indicate overall that correlated evolution across a number of anatomical characters has produced striking structural similarities in leaf anatomy among unrelated palm lineages. In the case of Caryoteae and Arecoideae, shared leaf anatomical characteristics, along with congruence in inflorescence architecture (e.g., flowers in triads), quite understandably led workers to include Caryoteae within Arecoideae (Uhl and Dransfield, 1987). Hence, one of the biggest surprises to emerge from molecular phylogenetic studies of palms is the unequivocal inclusion of the pinnate to bipinnate Caryoteae within Coryphoideae, and moreover, their resolution within a clade containing many fan palm genera of giant stature (syncarpous clade; Asmussen et al., 2006; Dransfield et al., 2008a, b).

But perhaps the most impressive instances of anatomical convergence occur between groups that are otherwise dissimilar and to which no close relationship has been attributed. These examples involve palms at ecological extremes within Coryphoideae, Ceroxyleae, and Attaleinae. Although convergence is well demonstrated in these taxa by their parallel evolution of fiber girders, it involves a broader suite of character states. *Ceroxylon* (Ceroxyleae) and *Parajubaea* (Attaleinae) show a complex organization of xeromorphic traits that are restricted to these quite unrelated genera. Both have well-developed stomatal furrows that are occluded by trichomes and positioned below longitudinal veins with well-developed fiber girders (Fig. 2K, L). Because these genera also contain the only palms occupying high elevations of the Andes, this unusual convergence deserves further investigation.

Tribe Cocoseae, which includes Attaleinae as one of three subtribes, are among the most distinctive lineages of pinnate-leaved palms, accorded subfamilial status within many classification schemes (formally or informally; Moore 1973) prior to the publication of the first *Genera Palmarum* (Uhl and Dransfield, 1987). Within this well-defined taxon, Tomlinson (1961) perceived a group congruent in circumscription with Attaleinae as one of the major, natural units within palms based on anatomical evidence and accorded them informal subfamilial status as the "Cocoid" palms in this restricted sense. Our results give this interpretation some resonance because the anatomy of many genera of Attaleinae is unusual within Arecoideae in being strongly convergent upon a suite of character states common within Coryphoideae. Genera such as *Attalea*, *Jubaeopsis*, and *Syagrus* revert from the cross-laminated surface layer type back to a parallel-laminated surface layer, and independently gain the transverse vein architecture and sheath type common within Coryphoideae. Anatomical convergence between the two groups is further demonstrated by the parallel gains of a multilayered hypodermis, which has a distribution within palms that is largely restricted to these groups (Tomlinson, 1961). But the most striking convergence between Attaleinae and Coryphoideae is the parallel gain of isobilateral lamina symmetry in *Butia* and several coryphoid genera (Fig. 2I, J).

Isobilateral lamina symmetry has long been suggested as evolving independently in multiple groups of palms (Koop, 1907; Tomlinson 1961)—an idea that is strongly supported by the results of this study (Fig. 10). Except for *Butia*, isobilateral leaves are distributed just within Coryphoideae, in which lamina symmetry lability is one of the predominant themes of anatomical evolution. That such a fundamental character as lamina symmetry is so evolutionarily labile is paradoxical; differences in symmetry involve a *suite* of structural differences throughout the leaf: the degree of complexity exhibited is similar to that mentioned for the xeromorphic Andean palms (e.g., *Ceroxylon, Parajubaea*). However, leaf developmental genetic studies offer a different perspective, indicating that polarity in leaves, and hence the fate of tissue symmetry is established with the inception of the leaf primordium (Eshed et al., 2001; Bowman et al., 2002). In maize leaves, *HD-ZIPIII* genes are critical to establishing polarity; expression mutants may have phenotypes in which leaf polarity is partially reversed, or in which (aside from the vascular bundles) both surfaces have either ad- or abaxial lamina histology (Timmermans et al., 1998; Juarez et al., 2004). Although the developmental genetics of isobilateral leaves are unknown, current knowledge suggests that polarity determination

in leaves is highly modular. Thus, the developmental "switch" between dorsiventral and isobilateral leaves may be quite labile, with a corresponding potential for change in lamina symmetry within lineages that possess the appropriate genetic capability.

Coryphoid palms certainly are such a lineage. Within the clade, taxa possessing isobilateral leaves are indigenous to open vegetation in (at least seasonally) dry climates (Dransfield et al., 2008b), habitats where this distinctive lamina histology may confer adaptive benefits (see our introduction and Smith et al., 1997; Evans and Vogelmann, 2006). Although we do not have data regarding the tempo of lamina symmetry change, a synthesis of such information with biogeographic and paleoclimatic data for coryphoids is desirable. Lamina symmetry evolution in Coryphoideae provides the clearest example in palms of the importance of anatomical diversification as a macroevolutionary mechanism for responding to change in the earth's climate over time.

Conclusions and future prospects—The present article is but a subset of a larger survey of the vegetative anatomy of palms that will be published as a separate volume by Oxford University Press. It serves as a model for the way in which anatomical information, derived from a study of all genera of palms, can be analyzed by an explicit methodology in combination with a robust phylogenetic understanding so that evolutionary trends within the family can be clearly perceived. We have shown that, despite extensive homoplasy, we can recognize that as palms have evolved there have been progressive changes in leaf anatomy. Some changes appear to be of biomechanical significance or otherwise have allowed palms to occupy drier habitats and higher latitudes and altitudes, so that they are no longer constrained by a tropical forest environment. To this ability, we have to add the consideration of the remarkable range of plant size that palms exhibit. This correlation of phylogenetic signal, growth habit, geographic distribution, and mechanics can be said to account for the many puzzling features of palm evolution. In applying this understanding, further work should add features of the anatomy of the leaf axis, stem, and root to the analysis. Our existing survey should allow us to do this.

LITERATURE CITED

ASMUSSEN, C. B., J. DRANSFIELD, V. DEICKMANN, A. S. BARFOD, J.-C. PINTAUD, AND W. J. BAKER. 2006. A new subfamily classification of the palm family (Arecaceae): Evidence from plastid DNA phylogeny. *Botanical Journal of the Linnean Society* 151: 15–38.

BAKER, W. J., AND S. ZONA. 2006. The palms: Preface. *Botanical Journal of the Linnean Society* 151: 2–3.

BAYTON, R. P. 2007. A revision of *Borassus* L. (Arecaceae). *Kew Bulletin* 62: 561–568.

BOWMAN, J. L., Y. ESHED, AND S. F. BAUM. 2002. Establishment of polarity in angiosperm lateral organs. *Trends in Genetics* 18: 134–141.

BRAKEFIELD, P. M. 2006. Evo-devo and constraints on selection. *Trends in Ecology & Evolution* 21: 362–368.

CASE, A. L., S. W. GRAHAM, T. D. MACFARLANE, AND S. C. H. BARRETT. 2008. A phylogenetic study of evolutionary transitions in sexual systems in Australasian *Wurmbea* (Colchicaceae). *International Journal of Plant Sciences* 169: 141–156.

CHABOT, B. F., AND D. J. HICKS. 1982. The ecology of leaf life spans. *Annual Review of Ecology and Systematics* 13: 229–259.

CHAPIN, F. S. III. 1989. The cost of tundra plant structures: Evaluation of concepts and currencies. *American Naturalist* 133: 1–19.

CHOONG, M. F., P. W. LUCAS, J. S. Y. ONG, B. PEREIRA, H. T. W. TAN, AND I. M. TURNER. 1992. Leaf fracture toughness and sclerophylly: Their correlations and ecological implications. *New Phytologist* 121: 597–610.

CUNNINGHAM, C. W., K. E. OMLAND, AND T. H. OAKLEY. 1998. Reconstructing ancestral character states: A critical reappraisal. *Trends in Ecology & Evolution* 13: 361–366.

DENGLER, N. G., R. E. DENGLER, AND D. R. KAPLAN. 1982. The mechanism of plication inception in palm leaves: Histogenetic observations on the pinnate leaf of *Chrysalidocarpus lutescens*. *Canadian Journal of Botany* 60: 2976–2998.

DONOGHUE, M. J., AND R. H. REE. 2000. Homoplasy and developmental constraints: A model and an example from plants. *American Zoologist* 40: 759–769.

DONOGHUE, M. J., AND M. J. SANDERSON. 1994. Complexity and homology in plants. *In* B. Hall [ed.], Homology: The hierarchical basis of comparative biology, 393–421. Academic Press, San Diego, California, USA.

DRANSFIELD, J., AND H. BEENTJE. 1995. The palms of Madagascar. Royal Botanic Gardens, Kew, UK.

DRANSFIELD, J., I. K. FERGUSON, AND N. W. UHL. 1990. The coryphoid palms: Patterns of variation and evolution. *Annals of the Missouri Botanical Garden* 77: 802–815.

DRANSFIELD, J., M. RAKOTOARINIVO, W. J. BAKER, R. P. BAYTON, J. B. FISHER, J. W. HORN, B. LEROY, AND X. METZ. 2008a. A new coryphoid palm genus from Madagascar. *Botanical Journal of the Linnean Society* 156: 79–91.

DRANSFIELD, J., N. W. UHL, C. B. ASMUSSEN, W. J. BAKER, M. M. HARLEY, AND C. E. LEWIS. 2005. A new phylogenetic classification of the palm family, Arecaceae. *Kew Bulletin* 60: 559–569.

DRANSFIELD, J., N. W. UHL, C. B. ASMUSSEN, W. J. BAKER, M. M. HARLEY, AND C. E. LEWIS. 2008b. Genera palmarum: The evolution and classification of palms. Royal Botanic Gardens, Kew, UK.

ESHED, Y., S. F. BAUM, J. V. PEREA, AND J. L. BOWMAN. 2001. Establishment of polarity in lateral organs of plants. *Current Biology* 11: 1251–1260.

EVANS, J. R., AND T. C. VOGELMANN. 2006. Photosynthesis within isobilateral *Eucalyptus pauciflora* leaves. *New Phytologist* 171: 771–782.

FAHN, A. 1954. The anatomical structure of the Xanthorrhoeaceae Dumort. *Botanical Journal of the Linnean Society* 55: 158–184.

FAHN, A. 1961. The anatomical structure of the Xanthorrhoeaceae Dumort. and its taxonomic position. *Recent Advances in Botany* 1: 155–160.

GARNIER, E., J.-L. SALAGER, G. LAURENT, AND L. SONIÉ. 1999. Relationships between photosynthesis, nitrogen and leaf structure in 14 grass species and their dependence on the basis of expression. *New Phytologist* 143: 119–129.

GIBSON, L. J., AND M. F. ASHBY. 1997. Cellular solids: Structure and properties, 2nd ed. Cambridge University Press, Cambridge, UK.

GIBSON, L. J., M. F. ASHBY, AND K. E. EASTERLING. 1988. Structure and mechanics of the iris leaf. *Journal of Materials Science* 23: 3041–3048.

GIRAUD-GUILLE, M. 1998. Plywood structures in nature. *Current Opinion in Solid State and Materials Science* 3: 221–227.

GIVNISH, T. 1979. On the adaptive significance of leaf form. *In* O. T. Solbrig, S. Jain, G. B. Johnson, and P. H. Raven [eds.], Topics in plant population biology, 373–407. Columbia University Press, New York, New York, USA.

GIVNISH, T. J., J. C. PIRES, S. W. GRAHAM, M. A. MCPHERSON, L. M. PRINCE, T. B. PATTERSON, H. S. RAI, ET AL. 2005. Repeated evolution of net venation and fleshy fruits among monocots in shaded habitats confirms *a priori* predictions: Evidence from an *ndhF* phylogeny. *Proceedings of the Royal Society of London, B, Biological Sciences* 272: 1481–1490.

HALLÉ, F. 1977. The longest leaf in palms? *Principes* 21: 18.

HALLÉ, F., R. A. A. OLDEMAN, AND P. B. TOMLINSON. 1978. Tropical trees and forests: An architectural analysis. Springer-Verlag, Berlin, Germany.

HENDERSON, A. 1990. Arecaceae. Part I. Introduction and the Iriarteinae. *Flora Neotropica* 53: 1–100.

HENDERSON, A., G. GALEANO, AND R. BERNAL. 1995. Field guide to palms of the Americas. Princeton University Press, Princeton, New Jersey, USA.

HODEL, D. R. 1992. Chamaedorea palms. The species and their cultivation. International Palm Society, Lawrence, Kansas, USA.

HOLMGREN, P. K., AND N. H. HOLMGREN. 1998 [continuously updated]. Index Herbariorum: A global directory of public herbaria and associated staff. New York Botanical Garden's Virtual Herbarium. Website http://sweetgum.nybg.org/ih [accessed March 2009].

JABBOUR, F., C. DAMERVAL, AND S. NADOT. 2008. Evolutionary trends in the flowers of Asteridae: Is polyandry an alternative to zygomorphy? *Annals of Botany* 102: 153–165.

JUAREZ, M. T., R. W. TWIGG, AND M. C. P. TIMMERMANS. 2004. Specification of adaxial cell fate during maize leaf development. *Development* 131: 4533–4544.

KAPLAN, D. R., N. G. DENGLER, AND R. E. DENGLER. 1982. The mechanism of plication inception in palm leaves: Histogenetic observations on the palmate leaf of *Rhapis excelsa. Canadian Journal of Botany* 60: 2999–3106.

KARABOURNIOTIS, G., J. F. BORNMAN, AND D. NIKOLOPOULOS. 2000. A possible optical role of the bundle sheath extensions of some heterobaric leaves of *Vitis vinifera* and *Quercus coccifera. Plant, Cell & Environment* 23: 423–430.

KENZO, T., T. ICHIE, Y. WATANABE, AND T. HIROMI. 2007. Ecological distribution of homobaric and heterobaric leaves in tree species of Malaysian lowland tropical rainforest. *American Journal of Botany* 94: 764–775.

KING, M. J., J. V. F. VINCENT, AND W. HARRIS. 1996. Curling and folding of leaves of monocotyledons—A strategy for structural stiffness. *New Zealand Journal of Botany* 34: 411–416.

KOOP, H. 1907. Anatomie des Palmenblattes mit besonderer Berücksichtigung ihrer Abhängigkeit von Klima und Standort. *Beihefte zum Botanischen Centralblatt* 22, Heft 1: 85–159.

LEEGOOD, R. C. 2008. Roles of the bundle sheath cells in leaves of C_3 plants. *Journal of Experimental Botany* 59: 1663–1673.

LEWIS, P. O. 2001. A likelihood approach to estimating phylogeny from discrete morphological character data. *Systematic Biology* 50: 913–925.

LUCAS, P. W., M. F. CHOONG, H. T. W. TAN, I. M. TURNER, AND A. J. BERRICK. 1991. The fracture toughness of the leaf of the dicotyledon *Calophyllum inophyllum* L. (Guttiferae). *Philosophical Transactions of the Royal Society of London, B, Biological Sciences* 334: 95–106.

MADDISON, W. P., AND D. R. MADDISON. 2006. StochChar: A package of Mesquite modules for stochastic character evolution, version 1.1. Website http://mesquiteproject.org [accessed June 2008].

MADDISON, W. P., AND D. R. MADDISON. 2008. Mesquite: A modular system for evolutionary analysis, version 2.5. Website http://mesquiteproject.org [accessed June 2008].

MEICENHEIMER, R. D., D. W. COFFIN, AND E. M. CHAPMAN. 2008. Anatomical basis for biophysical differences between *Pinus nigra* and *P. resinosa* (Pinaceae) leaves. *American Journal of Botany* 95: 1191–1198.

METCALFE, C. R. 1960. Anatomy of the monocotyledons, I. Gramineae. Oxford University Press, Oxford, UK.

MIDFORD, P., AND W. MADDISON. 2006. Correl package for Mesquite, version 0.1. Website http://mesquiteproject.org.

MOORE, H. E. JR. 1973. The major groups of palms and their distribution. *Gentes Herbarum* 11: 27–141.

MOTT, K. A., AND T. N. BUCKLEY. 2000. Patchy stomatal conductance: Emergent collective behavior of stomata. *Trends in Plant Science* 5: 258–262.

MOTT, K. A., A. C. GIBSON, AND J. W. O'LEARY. 1982. The adaptive significance of amphistomatic leaves. *Plant, Cell & Environment* 5: 455–460.

NIINEMETS, Ü., A. PORTSMUTH, D. TENA, M. TOBIAS, S. MATESANZ, AND F. VALLADARES. 2007. Do we underestimate the importance of leaf size in plant economics? Disproportional scaling of support costs within the spectrum of leaf physiognomy. *Annals of Botany* 100: 283–303.

NIKLAS, K. J. 1992. Plant biomechanics: An engineering approach to plant form and function. University of Chicago Press, Chicago, Illinois, USA.

NIKLAS, K. J. 1997. The evolutionary biology of plants. University of Chicago Press, Chicago, Illinois, USA.

NIKLAS, K. J. 1999. Research review: A mechanical perspective on foliage leaf form and function. *New Phytologist* 143: 19–31.

NIKOLOPOULOS, D., G. LIAKOPOULOS, I. DROSSOPOULOS, AND G. KARABOURNIOTIS. 2002. The relationship between anatomy and photosynthetic performance of heterobaric leaves. *Plant Physiology* 129: 235–243.

NOWAK, J., N. G. DENGLER, AND U. POSLUSZNY. 2007. The role of abscission during leaflet separation in *Chamaedorea elegans* (Arecaceae). *International Journal of Plant Sciences* 168: 533–545.

NOWAK, J., N. G. DENGLER, AND U. POSLUSZNY. 2008. Abscision-like leaflet separation in *Chamaedorea seifrizii* (Arecaceae). *International Journal of Plant Sciences* 169: 723–734.

PAGEL, M. 1994. Detecting correlated evolution on phylogenies: A general method for the comparative analysis of discrete characters. *Proceedings of the Royal Society of London, B, Biological Sciences* 255: 37–45.

POSADA, D., AND K. A. CRANDALL. 1998. MODELTEST: Testing the model of DNA substitution. *Bioinformatics* 14: 817–818. Website http://darwin.uvigo.es/software/modeltest.html.

READ, J., AND A. STOKES. 2006. Plant biomechanics in an ecological context. *American Journal of Botany* 93: 1546–1565.

READ, R. W. 1968. A study of *Pseudophoenix* (Palmae). *Gentes Herbarum* 10: 160–213.

RICH, P. M. 1987. Mechanical structure of the stem of arborescent palms. *Botanical Gazette* 148: 42–50.

ROTH-NEBELSICK, A., D. UHL, V. MOSBRUGGER, AND H. KERP. 2001. Evolution and function of leaf venation architecture: A review. *Annals of Botany* 87: 553–566.

RUNDEL, P. W., M. R. SHARIFI, A. C. GIBSON, AND K. J. ESLER. 1998. Structural and physiological adaptation to light environments in neotropical *Heliconia* (Heliconiaceae). *Journal of Tropical Ecology* 14: 789–801.

SACK, L., E. M. DIETRICH, C. M. STREETER, D. SÁNCHEZ-GÓMEZ, AND N. M. HOLBROOK. 2008. Leaf palmate venation and vascular redundancy confer tolerance of hydraulic disruption. *Proceedings of the National Academy of Sciences, USA* 105: 1567–1572.

SANDY, M., AND L. BACON. 2001. Tensile testing of raffia. *Journal of Materials Science Letters* 20: 529–530.

SANNIER, J., C. B. ASMUSSEN-LANGE, M. HARLEY, AND S. NADOT. 2007. Evolution of microsporogenesis in palms (Arecaceae). *International Journal of Plant Sciences* 168: 877–888.

SCHULTER, D., T. PRICE, A. O. MOOERS, AND D. LUDWIG. 1997. Likelihood of ancestor states in an adaptive radiation. *Evolution* 51: 1699–1711.

SCHWENDENER, S. 1874. Das mechanische Prinzip im anatomischen Bau der Monocotylen mit vergleichenden Ausblicken auf die übrigen Pflanzenklassen. W. Engelmann, Leipzig, Germany.

SLATON, M. R., AND W. K. SMITH. 2002. Mesophyll architecture and cell exposure to intercellular air spaces in alpine, desert, and forest species. *International Journal of Plant Sciences* 163: 937–948.

SMITH, W. K., T. C. VOGELMANN, E. H. DELUCIA, D. T. BELL, AND K. A. SHEPHERD. 1997. Leaf form and photosynthesis. *Bioscience* 47: 785–793.

SWOFFORD, D. L. 2002. PAUP*: Phylogenetic analysis using parsimony (*and other methods), version 4.0b10. Sinauer, Sunderland, Massachusetts, USA.

TERASHIMA, I. 1992. Anatomy of non-uniform leaf photosynthesis. *Photosynthesis Research* 31: 195–212.

TIMMERMANS, M. C. P., N. P. SCHULTES, J. P. JANKOVSKY, AND T. NELSON. 1998. *Leafbladeless1* is required for dorsoventrality of lateral organs in maize. *Development* 125: 2813–2823.

TOMLINSON, P. B. 1961. Anatomy of the monocotyledons. II. Palmae. Oxford University Press, Oxford, UK.

TOMLINSON, P. B. 1969. Anatomy of the monocotyledons. III. Commelinales-Zingiberales. Oxford University Press, Oxford, UK.

TOMLINSON, P. B. 1990. The structural biology of palms. Clarendon Press, Oxford, UK.

TOMLINSON, P. B. 2006. The uniqueness of palms. *Botanical Journal of the Linnean Society* 151: 5–14.

TOMLINSON, P. B., AND J. B. FISHER. 2005. Development of nonlignified fibers in leaves of *Gnetum gnemon. American Journal of Botany* 92: 383–389.

UHL, N. W., AND J. DRANSFIELD. 1987. Genera palmarum, 1st ed. L. H. Bailey Hortorium and International Palm Society, Lawrence, Kansas, USA.

VINCENT, J. F. 1982. The mechanical design of grass. *Journal of Materials Science* 17: 856–860.

VINCENT, J. F. 1991. Strength and fracture of grasses. *Journal of Materials Science* 26: 1947–1950.

VOGELMANN, T. C., AND G. MARTIN. 1993. The functional significance of palisade tissue: Penetration of directional versus diffuse light. *Plant, Cell & Environment* 16: 65–72.

VOGELMANN, T. C., J. N. NISHIO, AND W. K. SMITH. 1996. Leaves and light capture: Light propagation and gradients of carbon fixation within leaves. *Trends in Plant Science* 1: 65–71.

WRIGHT, I. J., AND M. WESTOBY. 2002. Leaves at low versus high rainfall: Coordination of structure, lifespan and physiology. *New Phytologist* 155: 403–416.

WRIGHT, I. J., P. B. REICH, M. WESTOBY, D. D. ACKERLY, Z. BARUCH, F. BONGERS, J. CAVENDER-BARES, ET AL. 2004. The worldwide leaf economics spectrum. *Nature* 428: 821–827.

WYLIE, R. B. 1952. Bundle sheath extension in the leaves of dicotyledons. *American Journal of Botany* 39: 645–651.

ZOBEL, D. B., AND V. T. LIU. 1980. Leaf-conductance patterns of seven palms in a common environment. *Botanical Gazette (Chicago, Ill.)* 141: 283–289.

ZONA, S. 1990. A monograph of *Sabal* (Arecaceae: Coryphoideae). *Aliso* 12: 583–666.

APPENDIX 1. Voucher information and data references for taxa examined in this study. Species examined that substitute those used in Asmussen et al. (2006) are listed in boldface type. Classification of subfamilies and tribes of Arecaceae follows Dransfield et al. (2008b). Genera and species within in each tribe are listed alphabetically. Herbarium acronyms follow Holmgren and Holmgren (1998). Plants cultivated at Fairchild Tropical Botanic Garden and the Montgomery Botanical Center have FTG and MBC, respectively, placed before the accession number.

Subfamily	Tribe	Taxon	Voucher information
Calamoideae	Eugeissoneae	*Eugeissona tristis* Griff.	*R.D. Worthington 13075* (FTG)
	Lepidocaryeae	*Eremospatha wendlandiana* Dammer ex Becc.	*T.C.H. Sunderland 1719* (BH)
		Korthalsia cheb Becc.	*J. Dransfield et al. JD 5876* (BH)
		Laccosperma acutiflorum (Becc.) J.Dransf.	*T.C.H. Sunderland 1755* (BH)
		Mauritia flexuosa L.f.	*L.R. Noblick 4944* (FTG)
		Oncocalamus tuleyi Sunderl.	*T.C.H. Sunderland 1759* (K)
		Raphia farinifera (Gaertn.) Hyl.	*J.W. Horn et al. 4928* (FTG)
	Calameae	*Calamus aruensis* Becc.	*R.A. Maturbongs 734* (K)
		***Metroxylon amicarum* (H.Wendl.) Hook.f.**	*J.W. Horn 4945* (PTBG)
		***M. upoluense* Becc.**	*H.E. Moore, Jr. 10398* (BH)
		***M. vitiense* (H.Wendl.) Hook.f.**	*K.M. Laubengayer KML 028* (FTG)
		Pigafetta elata (Mart.) H.Wendl.	*J.W. Horn 4941* (PTBG)
		Plectocomia mulleri Blume	*H.E. Moore, Jr. 9158 & W. Meijer* (BH)
		***Salacca magnifica* Mogea**	*J.W. Horn 4854* (FTG)
		***S. wallichiana* Mart.**	FTG 991677 B
		***S. zalacca* (Gaertn.) Voss**	FTG 2001–0864 A
Nypoideae		*Nypa fruticans* Wurmb	FTG 82473 B
Coryphoideae	Sabaleae	***Sabal causiarum* (O.F.Cook) Becc.**	*J.W. Horn 4780* (FTG)
		S. minor (Jacq.) Pers.	FTG RM765 C
	Cryosophileae	*Chelyocarpus ulei* Dammer	FTG 67291 A
		Coccothrinax argentata (Jacq.) L.H.Bailey	*J.W. Horn 4795* (FTG)
		Cryosophila warscewiczii (H.Wendl.) Bartlett	*J.W. Horn 4917* (FTG)
		Hemithrinax compacta (Griseb. & H.Wendl.) M.Gómez	*Léon 19542* (BH)
		Itaya amicorum H.E.Moore	*D. Bogler 1296* (FTG)
		Leucothrinax morrisii (H.Wendl.) C.E.Lewis & Zona	*P.R. Fantz 3208* (FTG)
		Schippia concolor Burret	*J.W. Horn 4836* (FTG)
		Thrinax radiata Lodd. ex Schult. & Schult.f.	FTG FG4897 B
		Trithrinax campestris (Burmeist.) Drude & Griseb.	*J.W. Horn 4853* (FTG)
		Zombia antillarum (Desc.) L.H.Bailey	*D. Bogler 1318* (FTG)
	Phoeniceae	*Phoenix canariensis* Chabaud	*J.W. Horn 4814* (FTG)
		P. dactylifera L.	FTG 93378
		P. reclinata Jacq.	*J.W. Horn 4809* (FTG)
	Trachycarpeae	*Acoelorraphe wrightii* (Griseb. & H.Wendl.) H.Wendl. ex Becc.	*W.M. Houghton 1054* (FTG)
		Brahea berlandieri Bartlett	*D. Bogler 1252* (FTG)
		Chamaerops humilis L.	*J.W. Horn 4810* (FTG)
		Colpothrinax wrightii Griseb. & H.Wendl. ex Voss	*D. Bogler 1278* (FTG)
		Copernicia prunifera (Mill.) H.E.Moore	*J.W. Horn 4799* (FTG)
		Guihaia argyrata (S.K.Lee & F.N.Wei) S.K.Lee, F.N.Wei & J.Dransf.	*D. Bogler 1294* (FTG)
		Johannesteijsmannia altifrons (Rchb.f. & Zoll.) H.E.Moore	*D. Bogler 1297* (FTG)
		***Licuala peltata* Roxb. ex Buch.-Ham.**	*J.W. Horn 4818* (FTG)
		***L. ramsayi* (F.Muell.) Domin**	*J.W. Horn 4930* (PTBG)
		***L. spinosa* Wurmb**	*L.R. Noblick 5198* (FTG)
		Livistona chinensis (Jacq.) R.Br. ex Mart.	*J.W. Horn 4837* (FTG)
		Maxburretia rupicola (Ridl.) Furtado	*H.E. Moore, Jr. et al. 9074* (BH)
		Pholidocarpus macrocarpus Becc.	*J.W. Horn et al. 4927* (FTG)
		Pritchardia arecina Becc.	*K.R. Wood 7991* (PTBG)
		P. pacifica Seem. & H.Wendl.	*J.W. Horn 4952* (PTBG)
		Pritchardiopsis jeanneneyi Becc.	*H.S. Mackee 38038* (FTG)
		Rhapidophyllum hystrix (Frazer ex Thouin) H.Wendl. & Drude	*S. Zona 900* (FTG)

APPENDIX 1. Continued.

Subfamily	Tribe	Taxon	Voucher information
		Rhapis excelsa (Thunb.) Henry	*J.W. Horn 4812* (FTG)
		Serenoa repens (W.Bartram) Small	*J.W. Horn 4794* (FTG)
		Trachycarpus fortunei (Hook.) H.Wendl.	*R.W. Read 780* (FTG)
		Washingtonia robusta H.Wendl.	*J.W. Horn 4852* (FTG)
	Chuniophoeniceae	*Chuniophoenix nana* Burret	*J.W. Horn 4796* (FTG)
		Kerriodoxa elegans J.Dransf.	*J.W. Horn 4930* (FTG)
		Nannorrhops ritchiana (Griff.) Aitch.	*J.B. Watson 1334* (FTG)
	Caryoteae	*Arenga hookeriana* (Becc.) Whitmore	*D.R. Hodel 1693 & P. Vatcharakorn* (BH)
		A. undulatifolia Becc.	FTG RM1715 A
		Caryota mitis Lour.	*S. Zona 920* (FTG)
		C. ophiopellis Dowe	MBC 98617 B
		Wallichia disticha T.Anderson	*J.W. Horn 4861A* (FTG)
	Corypheae	*Corypha taliera* Roxb.	MBC RM1144 E
		C. umbraculifera L.	*R. Sanders 1664* (FTG)
	Borasseae	*Bismarckia nobilis* Hildebr. & H.Wendl.	*P.R. Fantz 3668* (FTG)
		Borassodendron machadonis (Ridl.) Becc.	*J.W. Horn 4797* (FTG)
		Borassus flabellifer L.	*S. Zona 893* (FTG)
		Hyphaene thebaica (L.) Mart.	*L.R. Noblick 4911* (FTG)
		Latania verschaffeltii Lem.	FTG 60395 F
		Lodoicea maldivica (J.F.Gmel.) Pers. ex H.Wendl.	*H.E. Moore, Jr. 9037* (BH)
		Medemia argun (Mart.) Württemb. ex H.Wendl.	FTG 2000–830 B
		Satranala decussilvae Beentje & J.Dransf.	*H.J. Beentje 4474* (K)
Ceroxyloideae	Cyclospatheae	*Pseudophoenix sargentii* H.Wendl. ex Sarg.	*J.W. Horn 4813* (FTG)
		P. vinifera (Mart.) Becc.	FTG 81401 C
	Ceroxyleae	*Ceroxylon quindiuense* (H.Karst.) H.Wendl.	*J.W. Horn et al. 4866* (CAS)
		Juania australis (Mart.) Drude ex Hook.f.	*J.W. Horn et al. 4867* (CAS)
		Oraniopsis appendiculata (F.M.Bailey) J.Dransf.	*J.W. Horn et al. 4868* (CAS)
		***Ravenea glauca* Jum. & H.Perrier**	*C.E. Lewis CEL 01–099* (FTG)
		***R. hildebrandtii* H.Wendl. ex C.D.Bouché**	*J. French s.n.* (FTG)
		***R. rivularis* Jum. & H.Perrier**	*J.W. Horn 4819* (FTG)
	Phytelepheae	*Ammandra decasperma* O.F.Cook	*R.W. Sanders 1783* (FTG)
		Aphandra natalia (Balslev & A.J.Hend.) Barfod	*W. Quizhpe et al. 129* (FTG)
		Phytelephas macrocarpa Ruiz & Pav.	FTG 70279 A
		***P. seemannii* O.F.Cook**	*S. Zona 272* (RSA)
Arecoideae	Iriarteeae	*Dictyocaryum lamarckianum* (Mart.) H.Wendl.	*R. Bernal et al. 992* (FTG)
		Iriartea deltoidea Ruiz & Pav.	*W. Quizhpe et al. 920* (FTG)
		Iriartella stenocarpa Burret	*H.E. Moore, Jr. et al. 8455* (BH)
		Socratea exorrhiza (Mart.) H.Wendl.	*L.R. Noblick 5021* (FTG)
		Wettinia hirsuta Burret	*A. Henderson & H. Herrera 700* (FTG)
	Chamaedoreeae	*Chamaedorea microspadix* Burret	*T. Flynn 4259* (PTBG)
		Gaussia maya (O.F.Cook) H.J.Quero & Read	*C.E. Lewis CEL 00–001* (FTG)
		Hyophorbe lagenicaulis (L.H.Bailey) H.E.Moore	*P.R. Fantz 3297* (FTG)
		Synechanthus warscewiczianus H.Wendl.	*M. Calonje MAC06–15* (FTG)
		Wendlandiella gracilis (Burret) A.J.Hend.	*S. Zona 754* (FTG)
	Podococceae	*Podococcus barteri* G.Mann & H.Wendl.	*T.C.H. Sunderland 1803* (K)
	Oranieae	*Orania lauterbachiana* Becc.	*F.B. Essig & P. Katik LAE 55004* (BH)
		***O. trispatha* (J.Dransf. & N.W.Uhl) Beentje & J.Dransf.**	*H.E. Moore, Jr. 9921* (BH)
	Sclerospermeae	*Sclerosperma mannii* H.Wendl.	Data from Tomlinson (1961)
	Roystoneeae	*Roystonea oleracea* (Jacq.) O.F.Cook	*J.W. Horn 4924* (FTG)
	Reinhardtieae	*Reinhardtia simplex* (H.Wendl.) Burret	*J.W. Horn 4932* (PTBG)
	Cocoseae	*Acrocomia aculeata* (Jacq.) Lodd. ex Mart.	*J. Roncal 007* (FTG)
		A. crispa (Kunth) C.F.Baker ex Becc.	FTG 961365 C
		***Aiphanes horrida* (Jacq.) Burret**	*S. Zona 1093* (FTG)
		***A. minima* (Gaertn.) Burret**	*K. Laubengayer 1* (FTG)
		Allagoptera arenaria (M.Gómez) Kuntze	*P.R. Fantz 3543* (FTG)
		Attalea allenii H.E.Moore	*H.E. Moore, Jr. et al. 9460* (BH)
		Bactris gasipaes Kunth	*R.W. Sanders 1773 & W. Devia* (FTG)
		Beccariophoenix madagascariensis Jum. & H.Perrier	*S. Zona 1040* (FTG)
		Cocos nucifera L.	*J.W. Horn 4922* (FTG)
		Desmoncus orthacanthos Mart.	*H.E. Moore, Jr. et al. 10349* (BH)
		Elaeis guineensis Jacq.	*J.W. Horn 4834* (FTG)
		Jubaeopsis caffra Becc.	*W.F. Barker & E. E. Scheepe s.n.* (FTG)
		Syagrus smithii (H.E.Moore) Glassman	*H.E. Moore, Jr. et al. 8375* (BH)
		Voanioala gerardii J.Dransf.	*J. Dransfield et al. JD 6389* (BH)
	Manicarieae	*Manicaria saccifera* Gaertn.	*S. Zona 834* (FTG)
	Euterpeae	*Euterpe oleracea* Mart.	*L.R. Noblick 4964* (FTG)
		***Hyospathe elegans* Mart.**	FTG 91466 C
		Neonicholsonia watsonii Dammer	FTG FG2688 A
		***Prestoea pubigera* (Griseb. & H.Wendl.) Hook.f.**	*R. Sanders 1738* (FTG)

APPENDIX 1. Continued.

Subfamily	Tribe	Taxon	Voucher information
	Geonomateae	*Asterogyne martiana* (H.Wendl.) H.Wendl. ex Drude	*J.W. Horn 4860* (FTG)
		Calyptrogyne ghiesbreghtiana (Linden & H.Wendl.) H.Wendl.	*J.W. Horn 4873* (FTG)
		***Calyptronoma rivalis* (O.F.Cook) L.H.Bailey**	*S. Zona 864* (FTG)
		Geonoma congesta H.Wendl. ex Spruce	*R. Chazdon 23* (BH)
		Pholidostachys pulchra H.Wendl. ex Burret	*A. Henderson* & *H. Herrera 709* (FTG)
		Welfia regia H.Wendl.	FTG 8612 A
	Leopoldinieae	*Leopoldinia pulchra* Mart.	*G. Romero s.n.* (GH)
	Pelgodoxeae	*Pelagodoxa henryana* Becc.	*J.W. Horn 4956* (FTG)
		Sommieria leucophylla Becc.	FTG 2000308 A
	Areceae	*Acanthophoenix rubra* (Bory) H.Wendl.	*J.W. Horn 4915* (FTG)
		Actinokentia divaricata (Brongn.) Dammer	*L. Noblick 5207* (FTG)
		Actinorhytis calapparia (Blume) H.Wendl. & Drude ex Scheff.	*R. Kyburz K-PNG-W26* (FTG)
		Alloschmidia glabrata (Becc.) H.E.Moore	*J.-C. Pintaud et al. 468* (K)
		Archontophoenix purpurea Hodel & Dowe	*J.W. Horn 4817* (FTG)
		Areca triandra Roxb. ex Buch.-Ham.	*M.H. Chapin 033* (PTBG)
		***Balaka microcarpa* Burret**	*S. Zona* & *C. E. Lewis 993* (FTG)
		Basselinia velutina Becc.	*H.E. Moore, Jr. 10403* & *P. Morat* (BH)
		Bentinckia nicobarica (Kurz) Becc.	*S. Zona 796* (FTG)
		***Brassiophoenix drymophloeoides* Becc.**	*S. Zona 827* (FTG)
		Brongniartikentia lanuginosa H.E.Moore	*H.E. Moore, Jr. s.n.* (BH)
		Calyptrocalyx albertisianus Becc.	*S. Zona 891* (FTG)
		Campecarpus fulcitus (Brongn.) H.Wendl. ex Becc.	*H.E. Moore, Jr. 10413* (BH)
		Carpentaria acuminata (H.Wendl. & Drude) Becc.	*S. Zona 827* (FTG)
		Carpoxylon macrospermum H.Wendl. & Drude	FTG 961551 L
		Chambeyronia macrocarpa (Brongn.) Vieill. ex Becc.	FTG 94269 A
		Clinosperma bracteale (Brongn.) Becc.	*H.E. Moore, Jr. 10430* (FTG)
		Clinostigma savoryanum (Rehder & E.H.Wilson) H.E.Moore & Fosberg	*J.W. Horn 4934* (PTBG)
		Cyphokentia macrostachya Brongn.	*H.E. Moore, Jr. 10415* & *A. Cronquist* (BH)
		Cyphophoenix nucele H.E.Moore	FTG 74344 C
		Cyphosperma balansae (Brongn.) H.Wendl. ex Salomon	*H.E. Moore, Jr. et al. 10479* (FTG)
		Cyrtostachys renda Blume	*J.W. Horn 4816* (FTG)
		Dictyosperma album (Bory) Scheff.	*J.W. Horn 4838* (FTG)
		Dransfieldia micrantha (Becc.) W.J.Baker & Zona	FTG 98117 A
		Dypsis lutescens (H.Wendl.) Beentje & J.Dransf.	*J.W. Horn 4828* (FTG)
		Hedyscepe canterburyana (C.Moore & F.Muell.) H.Wendl. & Drude	*A. Rodd 1865* (BH)
		Heterospathe elata Scheff.	*S. Zona 613* (FTG)
		H. longipes (H.E.Moore) Norup	FTG 941037 A
		***Hydriastele pleurocarpa* (Burret) W.J.Baker & Loo**	*J.W. Horn 4913* (FTG)
		H. microspadix (Warb. ex K.Schum. & Lauterb.) Burret	FTG 79257 A
		Iguanura wallichiana (Mart.) Becc.	*J.W. Horn 4821* (FTG)
		Kentiopsis oliviformis (Brongn. & Gris) Brongn.	FTG 9168 A
		Laccospadix australasica H.Wendl. & Drude	*H.E. Moore, Jr. 9240* & *E. Volk* (BH)
		Lavoixia macrocarpa H.E.Moore	*H.E. Moore, Jr. 10464* (FTG)
		Lemurophoenix halleuxii J.Dransf.	*L.R. Noblick 5046* (FTG)
		Lepidorrhachis mooreana (F.Muell.) O.F.Cook	*H.E. Moore, Jr. 9250* & *M. Shick* (BH)
		Linospadix monostachya (Mart.) H.Wendl.	Harvard Forest slide
		Loxococcus rupicola (Thwaites) H.Wendl. & Drude	*R.W. Read* & *Jayasinghe 2399* (FTG)
		Marojejya darianii J.Dransf. & N.W.Uhl	FTG 2000827 A
		M. insignis Humbert	*H.E. Moore, Jr. 9901* (BH)
		Masoala kona Beentje	Not examined
		M. madagascariensis Jum.	*J. Dransfield JD 7634* (K)
		Moratia cerifera H.E.Moore	*H.E. Moore, Jr. 10400* (BH)
		Nenga pumila (Blume) H.Wendl.	*J.W. Horn 4804* (FTG)
		Neoveitchia storckii (H.Wendl.) Becc.	*J.W. Horn 4921* (FTG)
		Oncosperma tigillarium (Jack) Ridl.	*J.W. Horn 4857* (FTG)
		Phoenicophorium borsigianum (K.Koch) Stuntz	FTG 89205 A
		Physokentia petiolata (Burret) D.Fuller (=*P. rosea* H.E. Moore)	*H.E. Moore, Jr. et al. 10008* (BH)
		Ponapea ledermanniana Becc.	*S. Zona 878* (FTG)
		Ptychococcus paradoxus (Scheff.) Becc.	*J.W. Horn 4862* (FTG)
		Ptychosperma macarthurii (H.Wendl. ex H.J.Veitch) H.Wendl. ex Hook.f.	*S. Zona 869* (FTG)
		Rhopaloblaste augusta (Kurz) H.E.Moore	*J.W. Horn 4912* (FTG)
		Rhopalostylis baueri (Hook.f.) H.Wendl. & Drude	*J.W. Horn et al. 4863* (CAS)
		Roscheria melanochaetes (H.Wendl.) H.Wendl. ex Balf.f.	*J.W. Horn 4855* (FTG)
		Satakentia liukiuensis (Hatus.) H.E.Moore	*J.W. Horn 4825* (FTG)
		Tectiphiala ferox H.E.Moore	*H.E. Moore, Jr. et al. 10497* (K)
		Veillonia alba H.E.Moore	*L.R. Noblick 5212* (FTG)
		Veitchia arecina Becc.	*S. Zona 731* (FTG)
		Wodyetia bifurcata A.K.Irvine	*S. Zona 906* (FTG)

APPENDIX 1. Continued.

Subfamily	Tribe	Taxon	Voucher information
Outgroup family			
Bromeliaceae		*Vriesia psittacina* Lindl.	Data from Tomlinson (1969)
Cannaceae		*Canna edulis* Ker-Gawl.	Data from Tomlinson (1969)
Commelinaceae		*Tradescantia pallida* (Rose) D.R.Hunt	Data from Tomlinson (1969)
Dasypogonaceae		*Kingia australis* R.Br.	Data from Fahn (1961)
Dasypogonaceae		*Dasypogon bromelifolius* R.Br.	Data from Fahn (1954)
Haemodoraceae		***Anigozanthos flavidus* DC.**	*J. Fisher s.n.* (FTG)
Hanguanaceae		*Hanguana malayana* (Jack) Merr.	Data from Tomlinson (1969)
Musaceae		*Musa rosea* Baker	Data from Tomlinson (1969)
Poaceae		***Arundinaria* spp.**	Data from Metcalfe (1960)
Typhaceae		***Typha latifolia* L.**	*Brumbach 7486* (FTG)